Modeling cloud effects on hydrogen peroxide and methylhydroperoxide in the marine atmosphere

Cheol-Hee Kim and Sonia M. Kreidenweis
Department of Atmospheric Science, Colorado State University, Fort Collins, Colorado, USA

Graham Feingold
Environmental Technology Laboratory, NOAA, Boulder, Colorado, USA

Gregory J. Frost[1] and Michael K. Trainer
Aeronomy Laboratory, NOAA, Boulder, Colorado, USA

[1] Hydrogen peroxide (H_2O_2) and methylhydroperoxide (CH_3OOH) are studied with a coupled gas phase and aqueous phase chemical model representing a remote nonprecipitating cloudy boundary layer. Cloud interactions may deplete or enhance H_2O_2 but have a minor effect on CH_3OOH. Therefore two primary questions are addressed: (1) do nonprecipitating clouds perturb the ratio of H_2O_2/CH_3OOH, and if so, (2) what is the rate of reestablishment of this ratio to clear-sky levels following cloud contact. The results show that the rate of recovery of the ratio of H_2O_2 to CH_3OOH after perturbation by cloud interactions depends on NO_x (=NO + NO_2) mixing ratios and on the time of day that cloud is encountered. When cloud contact is followed by a significant period of daylight, recovery to precloud values is rapid; however, when cloud contact occurs during the late afternoon or night, recovery can take up to 24 hours under high NO_x conditions. Sensitivity tests show that in-cloud heterogeneous conversion of HNO_3 to aerosol has a small but detectable effect (~10%) on the recovery of the ratio. Neglecting dry deposition of H_2O_2 and HNO_3 increases the predicted ratio H_2O_2/CH_3OOH in clear air prior to cloud contact, and has a small effect on the relative recovery rate of the ratio. In-cloud consumption of H_2O_2 by SO_2 suppresses the postcloud ratio by ~40% relative to that in the base case for low levels of SO_2 (~200 ppt), with a more pronounced effect on the ratio and its rate of recovery for [SO_2] ~1 ppb. Because of the uncertainties associated with measurement of peroxides, and the dependence of the recovery of the ratio on the time of cloud contact, it is suggested that measurements of the ratio be considered judiciously and that they may not be of broad utility in predicting recent cloud contact. *INDEX TERMS:* 0365 Atmospheric Composition and Structure: Troposphere—composition and chemistry, 0320 Atmospheric Composition and Structure: Cloud physics and chemistry, 0322 Atmospheric Composition and Structure: Constituent sources and sinks; *KEYWORDS:* oxidants, aqueous chemistry, clouds, tropospheric chemistry

1. Introduction

[2] Hydrogen peroxide (H_2O_2) is considered an important oxidant due to its role in the free radical balance of the atmosphere and in the aqueous phase chemistry of acid precipitation. In recent years, considerable effort has been directed toward study of the heterogeneous production of sulfate. H_2O_2 and ozone (O_3) have been identified as the major oxidants responsible for the conversion of aqueous SO_2 to sulfate in cloud droplets [*Penkett et al.*, 1979; *Martin and Damschen*, 1981; *Kunen et al.*, 1983; *Maahs*, 1983; *Hegg*, 1989].

[3] Heterogeneous chemistry is important from a number of perspectives [*Ravishankara*, 1997]. First, drops can serve as a permanent sink of soluble gases if the drops fall to the surface. Second, soluble species may react within a drop at rates significantly higher than their gas-phase reaction rates. Third, the presence of clouds may alter the actinic flux and therefore gas-phase photolysis. Fourth, as noted above, heterogeneous chemistry can result in the formation of sulfate which modifies the aerosol size distribution that is released from cloud upon evaporation. These modified distributions can have a significant effect on light scattering [*Hegg et al.*, 1996] as well as on subsequent cloud formation [*Bower and Choularton*, 1993; *Feingold and Kreidenweis*, 2000]. Finally, and perhaps most relevant to our study, the presence of a cloud effectively separates soluble gases from insoluble gases and perturbs the balance of gas-phase chemistry [*Lelieveld and Crutzen*, 1991].

[4] In the remote marine atmosphere, H_2O_2 and methyl hydroperoxide (CH_3OOH) have been identified as interesting for a number of reasons. They play a central role in the oxidizing capacity of the atmosphere in remote regions [e.g., *Heikes et al.*, 1996]. Their fairly long lifetimes make them ideally suited to studies of diurnally averaged photochemistry [*Heikes et al.*, 1996]. Furthermore, H_2O_2 is very soluble (Henry's law constant of $7.45 \times 10^4 M$ atm^{-1} at 298 K), while CH_3OOH is much less soluble (Henry's law constant of $2.27 \times 10^2 M$ atm^{-1} at 298 K), so that the ratio of these peroxides should be a strong indicator of recent cloud contact. For example, *Cohan et al.* [1999] showed how in deep,
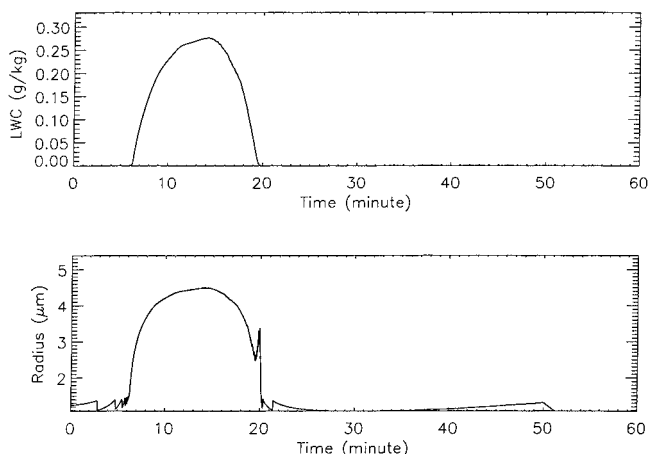
precipitating convective systems, H_2O_2 is significantly depleted, while CH_3OOH is not, and the ratio of H_2O_2/CH_3OOH (henceforth referred to as "the ratio") is reduced. The question of how this ratio behaves in nonprecipitating clouds (globally, the more prevalent situation) appears to be an open question.

[5] Several modeling approaches to the interaction of H_2O_2 and CH_3OOH with clouds have been taken [*Jacob*, 1986; *Chameides*, 1984; *Lelieveld and Crutzen*, 1991]. Research has pointed to the noticeable effect of cloud chemical processes on tropospheric photochemistry in the background atmosphere. *Lelieveld and Crutzen* [1991] pointed out that H_2O_2 concentrations in the background troposphere are significantly decreased by the presence of clouds. Some steady state gas phase photochemistry models have applied a constant, "heterogeneous loss" of H_2O_2 that is intended to account for surface deposition and cloud removal in the boundary layer (e.g., *Davis et al.* [1996] for the PEM-West A data). Other models have explicitly modeled the size-dependent uptake of H_2O_2 [e.g., *Chameides*, 1984; *Pandis and Seinfeld*, 1989; *Zhang et al.*, 1999] and have pointed to the importance of cloud water content drop size, and cloud contact time. Thus it is necessary to substantiate our understanding of the cloud effects controlling H_2O_2 and CH_3OOH levels with a detailed heterogeneous chemical model that includes these parameters.

[6] The goal of this study is to investigate how H_2O_2, CH_3OOH, and their ratio behave in nonprecipitating clouds in the remote troposphere, and to explore whether measurement of the ratio may aid in the interpretation of field data. To do this, we have coupled a gas phase model to a cloud model that simulates heterogeneous chemistry. The model is driven along the path of a kinematic trajectory in a stratocumulus-capped boundary layer, and parameters such as cloud liquid water content, drop size, and contact time are prescribed by the trajectory (Figure 1) [*Feingold et al.*, 1998], rather than by applying statistical data for mean cloud water content, mean drop size, and a prescribed contact time. These trajectories are derived from a simulation of a nonprecipitating marine stratocumulus cloudy boundary layer, and therefore results are only appropriate to that scenario. However, because stratocumulus clouds cover such extensive areas (annually averaged cloud cover 18 and 34% over land and ocean, respectively) and nonprecipitating clouds are the more common situation in the atmosphere, their role in cloud processing should be explored. To the extent that the details of cloud contact are important, the realistic cloud contact times represented in this model are expected to result in more accurate simulations of uptake on drops compared with a statistical approach.

[7] We present model results for a number of scenarios to examine the perturbation of the concentrations of H_2O_2 and CH_3OOH and their ratio through contact with a nonprecipitating cloud. The impact of daytime cloud contact versus nighttime cloud contact is contrasted. The effect on peroxide species of a sink of HNO_3 through permanent removal to the particulate phase as aerosol nitrate, and through dry deposition to the surface, is discussed. We also consider the role of SO_2 oxidation reactions in depletion of H_2O_2 and the role of chlorine chemistry. Results of this study provide insight into the importance of photochemical reactions and NO_x mixing ratios on the recovery of H_2O_2 and CH_3OOH concentrations following cloud contact.
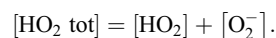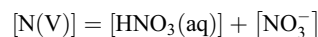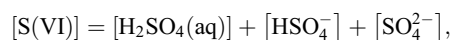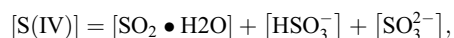
2. Heterogeneous Model Description

[8] We use a "box" model for stimulating the chemical processes that govern tropospheric heterogeneous chemistry. In order to investigate cloud-related effects in detail, gas-phase and aqueous-phase reactions as well as the transfer between the phases are considered. The coupled heterogeneous time-dependent box model is briefly presented in this section.

2.1. Gas Phase Chemistry

[9] The gas phase chemistry adopted in the generalized version of this model is based upon the mechanisms used in the steady state photochemical model of *Frost et al.* [1999]. The essential details of this model, along with the modifications and updates, can be found in the work of *McKeen et al.* [1997] and *Frost et al.* [1999]. The chemical mechanism contains various hydrocarbon classes and the detailed chemistry of most compounds known or expected to be present in the remote troposphere and has been used for modeling studies to simulate hydroxyl radicals and other species during photochemistry experiments [*McKeen et al.*, 1997; *Frost et al.*, 1999]. Here we have used a simplified version that does not initialize hydrocarbon species higher than CH_4. The resulting 14 gas phase species and 42 gas phase reactions, including 11 photolysis reactions are listed in Table 1. The rate constants were taken from *DeMore et al.* [1997], and the photolysis rate coefficients, or j values, were calculated using the Madronich radiative transfer model (RTM) (S. Madronich et al., Tropospheric ultraviolet-visible radiation model, Version 3.8, 1997, available at http://www.acd.ucar.edu/science/model.html), which is based upon the Stamnes discrete ordinates model [*Dahlback and Stamnes*, 1991]. The j values were interpolated for the actual zenith angle and altitudes [*Frost et al.*, 1999].

2.2. Aqueous Phase Chemistry

[10] The aqueous phase chemical mechanism is based on well-accepted models for uptake and aqueous mechanisms outlined in various references and texts [e.g., *Seinfeld and Pandis*, 1998; *Pandis and Seinfeld*, 1989]. Again, we have applied a simplified version for this work that comprises 49 individual aqueous phase species, 9 aqueous ionic equilibria, and 38 aqueous phase reactions. The reactant species in a particular class that are in rapid equilibrium in the aqueous phase are treated as the sum of these species [*Schwartz*, 1984; *Pandis and Seinfeld*, 1989], for example,

$$[S(IV)] = [SO_2 \bullet H2O] + [HSO_3^-] + [SO_3^{2-}],$$

$$[S(VI)] = [H_2SO_4(aq)] + [HSO_4^-] + [SO_4^{2-}],$$

$$[N(V)] = [HNO_3(aq)] + [NO_3^-]$$

$$[HO_2 \text{ tot}] = [HO_2] + [O_2^-].$$

In the absence of appropriate observations to initialize their aerosol and aqueous phase concentrations, we have chosen not to consider

Figure 1. Time history of liquid water content and droplet radius along parcel trajectory derived from large eddy simulation.

Table 1. Kinetic Data for Selected Gas Phase Reactions

Reaction	K_{298}[a]	$-\Delta H/R$, K
(R1) $HO_2 + HO_2 \rightarrow H_2O_2 + O_2$	3.7(−12)	
(R2) $CH_3O_2 + HO_2 \rightarrow CH_3OOH + O_2$	3.8(−13)	800
(R3) $O_3 \xrightarrow{h\nu} O(^1D) + O_2$	1.1(−4)[b]	
(R4) $O(^1D) + H_2O \rightarrow 2\ OH$	2.2(−10)	
(R5) $OH + CO \rightarrow HO_2 + CO_2$	1.5(−13)	
(R6) $OH + CH_4 \rightarrow CH_3O_2 + H_2O$	2.45(−12)	−1775
(R7) $HO_2 + O_3 \rightarrow OH + 2\ O_2$	1.1(−14)	−500
(R8) $OH + O_3 \rightarrow HO_2 + O_2$	1.6(−12)	−940
(R9) $HO_2 + NO \rightarrow NO_2 + OH$	3.5(−12)	250
(R10) $CH_3O_2 + NO \rightarrow HO_2 + CH_2O + NO_2$	3.0(−12)	280
(R11) $OH + NO_2 \rightarrow HNO_3$	1.1(−11)	
(R12) $HO_2 + NO_2 \rightarrow HO_2NO_2$	1.7(−12)	
(R13) $OH + H_2O_2 \rightarrow HO_2 + H_2O$	2.9(−12)	−160
(R14) $H_2O_2 \xrightarrow{h\nu} 2\ OH$	2.3(−5)[b]	
(R15) $OH + CH_3OOH \rightarrow 0.7\ CH_3O_2 + 0.3\ (CH_2O + OH)$	3.8(−12)	200
(R16) $CH_3OOH \xrightarrow{h\nu} HO_2 + OH + CH_2O$	1.6(−5)[b]	
(R17) $O(^1D)\ O_2 \rightarrow O + O_2$	2.97(−11)	
(R18) $O(^1D) + CH_4 \rightarrow CH_3O_2 + OH + H_2O$	1.5(−10)	
(R19) $O(^1D) + H_2 \rightarrow HO_2 + OH$	1.1(−10)	
(R20) $OH + H_2 \rightarrow HO_2 + HO_2$	5.5(−12)	−2000
(R21) $OH + HO_2 \rightarrow H_2O + O_2$	4.8(−11)	250
(R22) $NO + O_3 \rightarrow NO_2 + O_2$	2.0(−12)	−1400
(R23) $OH + HNO_3 \rightarrow H_2O + NO_3$	2.0(−13)	
(R24) $NO_3 + NO \rightarrow 2\ NO_2$	1.5(−11)	170
(R25) $NO_2 + O_3 \rightarrow NO_3$	1.2(−13)	−2450
(R26) $NO_3 + NO_2 \rightarrow N_2O_5$	1.4(−12)	
(R27) $N_2O_5 \rightarrow NO_3 + NO_2$	1.3(−3)	
(R28) $CH_3O_2 + CH_3O_2 \rightarrow 0.6\ H_2O + 1.2\ CH_2O$	2.5(−13)	190
(R29) $CH_2O + OH \rightarrow H_2O + HO_2 + CO$	1.0(−11)	
(R30) $OH + NO \rightarrow HONO$	8.2(−12)	
(R31) $NO + NO_2 + H_2O \rightarrow 2\ HONO$	6.0(−37)	
(R32) $N_2O_5 + H_2O \rightarrow 2HNO_3$	2.0(−21)	
(R33) $OH + HO_2NO_2 \rightarrow products$	1.3(−12)	380
(R34) $HO_2NO_2 \rightarrow HO_2 + NO_2$	3.0(−3)	
(R35) $NO_2 \xrightarrow{h\nu} NO + O$	2.3(−2)[b]	
(R36) $HNO_3 \xrightarrow{h\nu} OH + NO_2$	2.0(−6)[b]	
(R37) $CH_2O \xrightarrow{h\nu} 2\ HO_2 + CO$	1.4(−4)[b]	
(R38) $CH_2O \xrightarrow{h\nu} H_2 + CO$	9.6(−5)[b]	
(R39) $NO_3 \xrightarrow{h\nu} NO_2 + O$	0.5[b]	
(R40) $N_2O_5 \xrightarrow{h\nu} NO_3 + NO_2$	1.2(−4)[b]	
(R41) $HONO \xrightarrow{h\nu} OH + NO$	5.2(−3)[b]	
(R42) $HO_2NO_2 \xrightarrow{h\nu} HO_2 + NO_2$	1.5(−5)[b]	

[a] Units are s^{-1} for photolytic processes and molecules $cm^{-3}\ s^{-1}$ for two-body reactions.
[b] Photolysis rate constants (s^{-1}) are given at noontime.

the chemistry of trace metal ions, although their reactions may have considerable effect on HO_2 and other free radical concentrations [*Walcek et al.*, 1997].

2.3. Model Rate Expressions

[11] The dynamic processes between the aqueous phase and gas phase species are described by a set of mass balance differential equations. The general unit of concentration of the aqueous phase species is mol L^{-1} of water [*Pandis and Seinfeld*, 1989]. However, when liquid water content varies, it is convenient to use units for the aqueous phase concentrations of mol g^{-1} of air, yielding the following conservation equations:

$$\frac{d(C_i(g))}{dt} = -k_{mt}W_L C_i(g) + k_{mt}\frac{C_i(aq)}{K_H RT} + R_i \qquad (1)$$

$$\frac{d(C_i(aq))}{dt} = -k_{mt}W_L C_i(g) - k_{mt}\frac{C_i(aq)}{K_H RT} + R_i, \qquad (2)$$

where R_i is the net rate of production of species i by chemical reactions, k_{mt} ($= 3\eta\ D/r^2$ [*Pandis and Seinfeld*, 1989]) is a combined rate coefficient for gas phase plus interfacial mass transport, K_H is

the effective Henry's law constant, R is the ideal gas constant (0.08206 L atm/mol K), T is temperature (in kelvins), r is the cloud droplet radius (cm), and D is diffusivity in air ($cm^2\ s^{-1}$). The coefficient η is related to the sticking coefficient α and corrects for free molecular effects as approximated by *Fuchs and Sutugin* [1971], and W_L is the cloud liquid water content (L water/L air). Values for the diffusion constant D are not known for all gases, but a value of 0.1 $cm^2\ s^{-1}$ is assumed to be representative for most species [*Schwartz*, 1986]. Values of D and of the dimensionless accommodation or sticking coefficients, α, used in this work are shown in Table 2. The model assumes that the drop population is represented by a single, time-varying mean drop size for the calculation of the mass transfer rates. The time-dependent mean drop size was computed in the parent LES simulation based on input aerosol concentrations and depends on the liquid water content and kinetic growth of droplets.

3. Peroxide Chemistry in the Marine Environment

[12] The H_2O_2 and CH_3OOH concentrations are mainly controlled by the mixing ratios of O_3, CO, NO_x, and H_2O and the UV radiation intensity [*McElroy*, 1986]. The important sinks are

Table 2. Sticking and Coefficients and Diffusion Coefficients Used in This Work[a]

Species	Sticking Coefficient	Diffusion Coefficient, $cm^2 \ s^{-1}$	Reference
NO	0.05	0.1	*Lelieveld and Crutzen* [1991]
NO_2	6.3×10^{-4}	0.1	*Tang and Lee* [1987]
NO_3	1.0×10^{-3}	0.1	*Thomas et al.* [1989]
O_3	5.3×10^{-4b}	0.1	*Tang and Lee* [1987]
OH	0.5[c]	0.229	*Frost et al.* [1999]
HO_2	0.01[d]	0.175	*Frost et al.* [1999]
H_2O_2	0.18	0.1	*JPL* [1997]
CH_3OOH	0.05	0.1	*Lelieveld and Crutzen* [1991]
HNO_3	0.2	0.1	*DeMore et al.* [1997]
CH_2O	0.04	0.1	*DeMore et al.* [1997]
CH_3O_2	0.01	0.1	*Lelieveld and Crutzen* [1991]
HNO_2	0.5	0.13	*DeMore et al.* [1997]
HCl	0.01	0.1	*Lelieveld and Crutzen* [1991]
SO_2	0.035[e]	0.1	*Gardner et al.* [1987]

[a] Here 0.01 and 0.1 $cm^2 \ s^{-1}$ were adopted as sticking coefficient and diffusion coefficient, respectively, for the other species unless noted.
[b] Here $1.5 \times 10^{-5} \ cm^2 \ s^{-1}$ was used for aqueous phase diffusion coefficient.
[c] Range of reported values, $0.0035 \sim 1$.
[d] Range of reported values, $0.01 \sim 1$.
[e] Range of reported values, $0.02 \sim 0.05$.

heterogeneous loss (wet and dry deposition), aqueous phase conversion, homogeneous gas phase oxidation by OH, and photolysis [*Herrmann et al.*, 1999]. In this section we describe the general chemistry and summarize some reported observations of H_2O_2 and CH_3OOH.

### 3.1. Production and Loss of Peroxides in Gas Phase Chemistry

[13] In the troposphere, gas phase reactions of HO_2 and CH_3O_2 radicals produce H_2O_2 and CH_3OOH:

(R1) $\qquad HO_2 + HO_2 \quad \rightarrow \quad H_2O_2 + O_2$

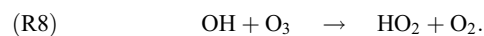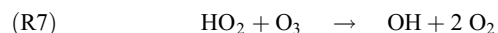(R2) $\qquad CH_3O_2 + HO_2 \quad \rightarrow \quad CH_3OOH + O_2.$
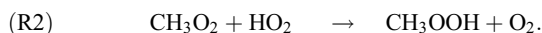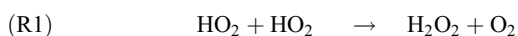
[14] The production of HO_2 in the troposphere can be described as a HO_x-catalyzed chain oxidation of carbon monoxide [e.g., *Thompson and Cicerone*, 1986; *Schwartz*, 1984]. The chain is initiated by production of HO_2 pricipally from hydroxyl radicals:

(R3) $\qquad O_3 + hv \quad \rightarrow \quad O_2 + O(^1D)$

(R4) $\qquad O(^1D) + H_2O \quad \rightarrow \quad 2 \ OH.$
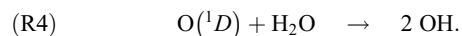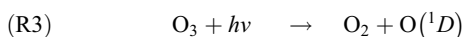
[15] In remote marine areas (where there are no significant sources of VOCs), OH is removed by reaction with CO and CH_4, and in the presence of O_2 this leads to the formation of HO_2 and CH_3O_2:

(R5) $\qquad OH + CO + O_2 \quad \rightarrow \quad HO_2 + CO_2$

(R6) $\qquad OH + CH_4 + O_2 \quad \rightarrow \quad CHO_3O_2 + H_2O.$
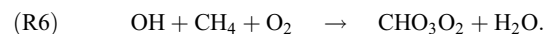
[16] Both HO_2 and OH can react with O_3:

(R7) $\qquad HO_2 + O_3 \quad \rightarrow \quad OH + 2 \ O_2$

(R8) $\qquad OH + O_3 \quad \rightarrow \quad HO_2 + O_2.$

[17] However, when sufficient concentrations of NO are present, HO_2 and CH_3O_2 both react with NO:

(R9) $\qquad HO_2 + NO \quad \rightarrow \quad NO_2 + OH$

(R10) $\qquad CH_3O_2 + NO + O_2 \quad \rightarrow \quad CH_2O + NO_2 + HO_2.$
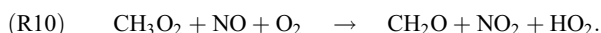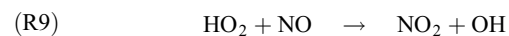
NO_2 pholyzes to $O(^3P)$, which adds to O_2 to form O_3.

[18] While OH and HO_2 are recyled in these reactions, they are removed at higher NO_x concentrations by reactions with NO_2, forming nitric and pernitric acids:
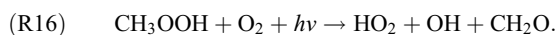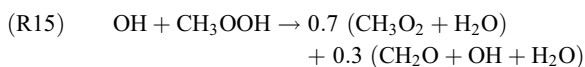
(R11) $\qquad OH + NO_2 \quad \rightarrow \quad HNO_3$

(R12) $\qquad HO_2 + NO_2 \quad \longleftrightarrow \quad HO_2NO_2.$
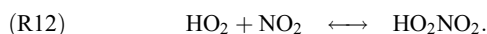
[19] The main gas-phase losses of H_2O_2 are through its photolysis and its reaction with OH,

(R13) $\qquad OH + H_2O_2 \quad \rightarrow \quad HO_2 + H_2O$

(R14) $\qquad H_2O_2 + hv \quad \rightarrow \quad 2 \ OH.$
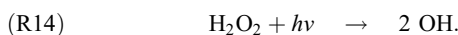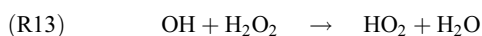
Reaction (R13) cycles HO_x ($HO_x = OH + HO_2$), whereas (R14) regenerates HO_x.

[20] The primary loss mechanism of CH_3OOH in the gas phase is similar to that for H_2O_2:

(R15) $\qquad OH + CH_3OOH \rightarrow 0.7 \ (CH_3O_2 + H_2O)$
$\qquad\qquad\qquad\qquad\qquad + 0.3 \ (CH_2O + OH + H_2O)$

(R16) $\qquad CH_3OOH + O_2 + hv \rightarrow HO_2 + OH + CH_2O.$

[21] Field measurements of H_2O_2 and CH_3OOH have been performed over the years and analyzed as a function of latitude/longitude, altitude, and various other parameters in continental and marine areas [*Jacob et al.*, 1990; *Jacob and Klockow*, 1992; *Heikes*, 1992; *Thompson et al.*, 1993]. Measurements of H_2O_2 prior to 1993 are summarized by *Martin et al.* [1997]. H_2O_2 concentrations observed in the troposphere are typically about $1 \sim 5$ ppb [e.g., *Daum et al.*, 1990; *Tremmel et al.*, 1993; *Macdonald et al.*, 1995; *Staffelbach et al.*, 1996; *Martin et al.*, 1997]. The concentrations of H_2O_2 in remote areas are not very different from those in more polluted urban areas. For example, *Heikes et al.* [1996] reported levels of $0.3 \sim 5$ ppb in the marine boundary layer, and *Weinstein-Lloyd et al.* [1998] measured con-

Table 3. Henry's Law Constants and Aqueous Phase Equilibrium Reactions

	K_{298},[a] M or M atm^{-1}	$-\Delta H/R$, K	Reference
	Henry's Law Constants		
(H1) O_3	1.13(−2)[b]	2300	*Kozac-Channing and Heltz* [1983]
(H2) OH	2.5(1)	5280	*Jacob* [1986]
(H3) HO_2	2.0(3)	6640	*Jacob* [1986]
(H4) H_2O_2	7.5(4)	6620	*Lind and Kok* [1986]
(H5) CH_3OOH	2.27(2)	5610	*Lind and Kok* [1986]
(H6) HCHO	6.3(3)	6460	*Ledbury and Blair* [1925]
(H7) NO	1.9(−3)	1480	*Schwartz and White* [1981]
(H8) NO_2	1.00(−2)	2500	*Schwartz* [1984]
(H9) NO_3	2.1(5)	8700	*Jacob* [1986]
(H10) HNO_3	2.1(5)		*Schwartz* [1984]
(H11) CO_2	3.4(−2)	2420	*Smith and Martell* [1976]
(H12) HNO_2	4.9(1)	4780	*Schwartz and White* [1981]
(H13) CH_3O_2	6.0(0)	5600	*Jacob* [1986]
(H14) HCOOH	3.5(3)	5740	*Latimer* [1952]
	Equilibrium Reactions		
(E1) $H_2O_2(aq) \rightleftharpoons HO_2^- + H^+$	2.2(−12)	−3730	*Smith and Martell* [1976]
(E2) $HNO_3(aq) \rightleftharpoons NO_3^- + H^+$	1.54(1)	8700	*Schwartz* [1984]
(E3) $HNO_2(aq) \rightleftharpoons NO_2^- + H^+$	5.1(−4)	−1260	*Schwartz and White* [1981]
(E4) $CO_2 \cdot H_2O \rightleftharpoons HCO_3^- + H^+$	4.46(−7)	−1000	*Smith and Martell* [1976]
(E5) $HCO_3 \rightleftharpoons CO_3^{2-} + H^+$	4.68(−11)	−1760	*Smith and Martell* [1976]
(E6) $H_2O \rightleftharpoons H^+ + OH^-$	1.0(−14)	−6710	*Smith and Martell* [1976]
(E7) $HCHO(aq) + H_2O \rightleftharpoons H_2C(OH)_2(aq)$	1.82(3)	4020	*Le Henaff* [1968]
(E8) $HCOOH(aq) \rightleftharpoons HCOO^- + H^+$	1.78(−4)	−20	*Martell and Smith* [1977]
(E9) $HO_2(aq) \rightleftharpoons H^+ + O_2^-$	3.50(−5)		*Perrin* [1982]

[a] The temperature dependence is represented by $K = K_{298} \exp \{\Delta H/R[(1/T) - (1/298)]\}$, where K is the equilibrium constant at temperature T.
[b] Note: Read 1.13(−2) as 1.13×10^{-2}.

centrations of 1 ∼ 4 pbb in the continental boundary layer at midday in a rural area in the southern United States. The reason is that although there is a great deal more photochemical activity in the polluted areas, which might be expected to lead to enhanced H_2O_2, there is also more NO. Since H_2O_2 is formed by (R1) and HO_2 also reacts rapidly with NO via (R9), higher NO_x levels tend to inhibit the formation of H_2O_2. Some measurements of CH_3OOH have also been reported. Typical marine concentrations of CH_3OOH are 0.1 ∼ 0.5 ppb, although concentrations as high as 1.6 ppb have been observed in remote areas [*Staffelbach et al.*, 1996]. Throughout the troposphere, CH_3OOH has generally been observed at smaller concentrations than H_2O_2 [*O'Sullivan et al.*, 1999].

[22] Ratios of $[H_2O_2]/[CH_3OOH]$ observed in the NASA Global Tropospheric Experiment, Pacific Exploratory Missions (GTE-PEM), 1991–1996, were reported by *O'Sullivan et al.* [1999]. Values of the ratio >6 were observed in elevated continental outflow layers, while ratios >2 were found in some regions affected by pollution plumes. The median ratio from 45°S to 35°N, 0 to 4 km, was between 1 and 2, except near the ITCZ where removal of H_2O_2 led to ratios <1. The ratio generally increased with altitude. There are several reasons for this vertical dependence: loss of H_2O_2 via dry deposition is effective in the boundary layer; the rate coefficient of the reaction OH + CH_4, which leads to CH_3O_2 production, decreases with decreasing temperature; and NO_x tends to be higher in the upper troposphere than in the marine boundary layer. This work explores the potential for interactions with nonprecipitating clouds to also perturb observed ratios of $[H_2O_2]/[CH_3OOH]$.

3.2. Aqueous Phase Chemistry of H_2O_2 and CH_3OOH

[23] The important equilibrium and kinetic reactions associated with H_2O_2 and CH_3OOH are given in Tables 3 and 4 [*Jacob*, 1986; *Chameides*, 1984; *McElroy*, 1986]. Cloud contact tends to reduce [OH] and [HO_2], but by different pathways, if *j* values are assumed to be similar to those in clear air. Gas-phase production of OH(g) is

slowed in cloud because an important gas phase source of OH(g) (via reaction (R9)) is reduced by the rapid uptake of HO_2 into cloud water. However, the major gas phase sinks, (R5) and (R6), are little affected by cloud because CO and CH_4 are not soluble. Loss of OH(g) by transfer to the aqueous phase is slower than the gas phase OH(g) sinks and has only a minor effect on [OH(g)]. On the other hand, the HO_2 radical is more soluble than OH (Henry's law constant of 4.3×10^3 M atm^{-1} at 298 K compared with 25 M atm^{-1} for OH), and HO_2 is efficiently scavengend by cloud droplets. Its solubility is further enhanced by acid-base dissociation of $HO_2(aq)$(reaction (E9)), and $HO_2(tot)$ (=$HO_2 + O_2^-$) is primarily removed by reactions (A7), (A13), and (A35) (Table 4).

[24] Since peroxide concentrations are linked to [OH] and [HO_2], and H_2O_2 itself is very soluble, [H_2O_2(g)] is also reduced in cloud, and its counterpart H_2O_2(aq) can be destroyed by several aqueous-phase reactions. (We do not consider aqueous-phase reaction with SO_2, which can be an important sink for H_2O_2, in our base case, but do examine its effect in a sensitivity study discussed later.) However, (A2), (A6), (A7), (A8), and (A14) produce H_2O_2(aq) that can be degassed when the cloud evaporates, and thus the cloud can be a net source of H_2O_2(g) in some situations. In particular, the dominant in-cloud H_2O_2-producing reaction, (A7), is most rapid at pH ∼4.5, where [O_2^-] ≈ [HO_2]. The importance of aqueous phase H_2O_2 production has been discussed in detail by *Chameides* [1984] and *Jacob* [1986].

[25] The cloud effect on CH_3OOH can also be complex. The Henry's law constant for its precursor, CH_3O_2, is estimated to be of order unity (H13), so that the droplets do not constitute a significant direct CH_3O_2(g) sink. Production of CH_3O_2(g) through reaction (R6) in cloudy air is slower than before cloud formation because of the lower OH(g) concentrations, whereas the gas-phase destruction of CH_3O_2(g) by NO(g) is not inhibited by cloud formation due to the low solubility of NO. Thus the gas-phase reaction of CH_3O_2(g) with HO_2(g) to produce CH_3OOH(g) is inhibited by depletion of both radicals. On the other hand, CH_3O_2 (aq) will react rapidly with O_2^- via (A35) to produce CH_3OOH(aq). The CH_3OOH(aq) is outgassed due to its

Table 4. Kinetic Data for Selected Aqueous Phase Reactions

Reaction	K_{298}, M or M atm^{-1}	$-\Delta H / R$, K	Reference
(A1) $H_2O_2 \xrightarrow{hv,} 2\ OH$	$1.28(-5)^a$		*Graedel and Weschler* [1981]
(A2) $O_3 \xrightarrow{hv,\ H_2O} H_2O_2 + O_2$	$2.0(-4)^a$		*Graedel and Weschler* [1981]
(A3) $OH + HO_2 \rightarrow H_2O + O_2$	$7.0(9)$	-1500	*Sehested et al.* [1968]
(A4) $OH + O_2^- \rightarrow OH^- + O_2$	$1.0(10)$	-1500	*Sehested et al.* [1968]
(A5) $OH + H_2O_2 \rightarrow H_2O + HO_2$	$2.7(7)$	-1700	*Christensen et al.* [1982]
(A6) $HO_2 + HO_2 \rightarrow H_2O_2 + O_2$	$8.6(5)$	-2365	*Bielski* [1978]
(A7) $HO_2 + O_2^- \xrightarrow{H_2O} H_2O_2 + O_2 + OH^-$	$1.0(8)$	-1500	*Bielski* [1978]
(A8) $O_2^- + O_2^- \xrightarrow{2H_2O} H_2O_2 + O_2 + 2\ OH^-$	<0.3		*Bielski* [1978]
(A9) $HO_2 + H_2O_2 \rightarrow OH + O_2 + H_2O$	0.5		*Weinstein and Bielski* [1979]
(A10) $O_2^- + H_2O_2 \rightarrow OH + O_2 + OH^-$	0.13		*Weinstein and Bielski* [1979]
(A11) $OH + O_3 \rightarrow HO_2 + O_2$	$2(9)$		*Staehelin and Hoigne* [1982]
(A12) $HO_2 + O_3 \rightarrow OH + 2\ O_2$	$<1(4)$		*Sehested et al.* [1984]
(A13) $O_2^- + O_3 \xrightarrow{H_2O} OH + 2\ O_2 + OH^-$	$1.5(9)$	-1500	*Sehested et al.* [1984]
(A14) $OH^- + O_3 \xrightarrow{H_2O} H_2O_2 + O_2 + OH^-$	70		*Staehelin and Hoigne* [1982]
(A15) $HO_2^- + O_3 \rightarrow OH + O_2^- + O_2$	$2.8(6)$		*Staehelin and Hoigne* [1982]
(A16) $H_2O_2 + O_3 \rightarrow H_2O + 2\ O_2$	$7.8(-3)[O_3]^{-0.5}$		*Martin* [1984]
(A17) $H_2O_2 + NO_3 \rightarrow NO_3^- + H^+ + HO_2$	$1.0(6)$	-2800	*Chameides* [1984]
(A18) $HCO_3^- + OH \rightarrow H_2O + CO_3^-$	$1.5(7)$	-1910	*Weeks and Rabani* [1966]
(A19) $HCO_3^- + O_2^- \rightarrow HO_2^- + CO_3^-$	$1.5(6)$		*Schmidt* [1972]
(A20) $CO_3^- + O_2^- \xrightarrow{H_2O} HCO_3^- + O_2 + OH^-$	$4.0(8)$	-1500	*Behar et al.* [1970]
(A21) $CO_3^- + H_2O_2 \rightarrow HO_2 + HCO_3^-$	$8.0(5)$	-2820	*Behar et al.* [1970]
(A22) $H_2C(OH)_2 + OH \xrightarrow{O_2} HCOOH + HO_2 + H_2O$	$2.0(9)$	-1500	*Bothe and Schulte-Frohlinde* [1980]
(A23) $H_2C(OH)_2 + O_3 \rightarrow H_2O + products$	0.1		*Hoigne and Bader* [1983a]
(A24) $HCOOH + OH \xrightarrow{O_2} CO_2 + HO_2 + H_2O$	$2.0(8)$	-1500	*Scholes and Willson* [1967]
(A25) $HCOOH + H_2O_2 \rightarrow H_2O + products$	$4.6(-6)$	-5180	*Shapilov and Kostyukovskii* [1974]
(A26) $HCOOH + NO_3 \xrightarrow{O_2} NO_3^- + H^+ + CO_2 + HO_2$	$2.1(5)$	-3200	*Dogliotti and Hayon* [1967]
(A27) $HCOOH + O_3 \rightarrow CO_2 + HO_2 + OH$	5.0		*Hoigne and Bader* [1983b]
(A28) $HCOOH + Cl_2^- \xrightarrow{O_2} CO_2 + HO_2 + 2\ Cl^- + H^+$	$6.7(3)$	-4300	*Hagesawa and Neta* [1978]
(A29) $HCOO^- + OH \xrightarrow{O_2} CO_2 + HO_2 + OH^-$	$2.5(9)$	-1500	*Anbar and Neta* [1967]
(A30) $HCOO^- + O_3 \rightarrow CO_2 + OH + O_2^-$	100.0		*Hoigne and Bader* [1983b]
(A31) $HCOO^- + NO_3 \xrightarrow{O_2} NO_3^- + CO_2 + HO_2$	$6.0(7)$	-1500	*Jacob* [1986]
(A32) $HCOO^- + CO_3^- \xrightarrow{O_2H_2O} CO_2 + HCO_3^- + HO_2$	$1.1(5)$	-3400	*Chen et al.* [1973]
(A33) $HCOO^- + Cl_2^- \xrightarrow{O_2} CO_2 + HO_2 + 2Cl^-$	$1.9(6)$	-2600	*Hagesawa and Neta* [1978]
(A34) $CH_3O_2 + HO_2 \rightarrow CH_3OOH + O_2$	$4.3(5)$	-3000	*Jacob* [1986]
(A35) $CH_3O_2 + O_2^- \xrightarrow{H_2O} CH_3OOH + O_2 + OH^-$	$5.0(7)$	-1600	*Jacob* [1986]
(A36) $CH_3OOH \xrightarrow{hv\ H_2O} HCHO + OH + HO_2$	$1.59(-5)^a$		*Graedel and Weschler* [1981]
(A37) $CH_3OOH + OH \rightarrow CH_3O_2 + H_2O$	$2.7(7)$	-1700	*Jacob* [1986]
(A38) $CH_3OOH + OH \rightarrow HCHO + OH + H_2O$	$1.9(7)$	-1800	*Anbar and Neta* [1967]

[a] Photolysis rate constants (s^{-1}) are given at noontime.

low solubility, resulting in an in-cloud increase in $CH_3OOH(g)$. Since it involves the radical species CH_3O_2 and HO_2, this production pathway is active only in the daytime and is important at relatively high pH (pH > 4.5).

4. Results

4.1. Results From Gas Phase Steady State Chemistry

[26] As a first step in exploring the behavior of peroxides and the impact of clouds, we investigated the response of gas-phase $[H_2O_2]$ and $[CH_3OOH]$ to changes in photochemical environment. A series of gas phase only simulations were run to a diurnal steady state under a wide range of fixed concentrations of O_3 (15 ppb ~ 65 ppb) and NO_x (5 ~ 1000 ppt), and applying a constant dry deposition velocity of 1 cm s^{-1} (loss timescale is 10^5 s) for both H_2O_2 and HNO_3 [*Seinfeld and Pandis*, 1998]. Other initial and fixed conditions, chosen to represent the summertime Southern Ocean environment, are shown in Table 5. These simulations yield an overview of the role of HO_x/NO_x reactions in controlling $[H_2O_2]$ and $[CH_3OOH]$. The results were also used to calculate a "missing" NO_x source [e.g., *Lelieveld and Crutzen*, 1991; *Liu et al.*, 1992] required to maintain approximately constant NO_x levels during the subsequent 4-day runs described below. In the real atmosphere this source can be attributed to lightning or advection from regions characterized by higher NO_x concentration.

Although fixing, or applying artificial NO_x sources, creates an idealized situation, it does allow us to use NO_x as an independent variable and explore the response of the system to changes in NO_x. The NO_x emission rates implied by this procedure are 0.2, 4.0, and 71.3 ppt h^{-1} for NO_x = 5, 50, and 500 ppt, respectively. *Price et al.* [1997] estimated the global mean lightning source of tropospheric NO_x as ~0.5 ppt h^{-1} which is significantly lower than the assumed rates for NO_x = 50 and 500 ppt. However, one should bear in mind that data on lightning sources of NO_x over the ocean are sparse and unreliable, and that global mean values may be much lower than local sources, for example, near the outflow from convective storms. Further, advection of NO_x reservoir species from continental regions could also contribute to the implied NO_x source.

[27] Figure 2 shows the noontime concentrations of various species as functions of $[NO_x]$ and $[O_3]$, as predicted by the steady state, gas-phase only simulations. The concentration of OH (Figure 2a) increases with NO_x for NO_x less than 1000 ppt due to the increasing conversion of HO_2 to OH by NO [*Logan et al.*, 1981]. Relatively high NO_x concentrations play an important role in the budget of gaseous OH through reaction (R9), whereas the main loss of OH (reactions (R5) and (R6)) is not sensitive to NO_x concentration levels. The primary source of HO_2 at low $[NO_x]$ (Figure 2b) is the OH conversation process through reaction (R5). The addition of NO_x increases the HO_2 production rate through (R10) and increases OH conversion reactions (reactions (R5) or (R8)). However, the loss of HO_2 through (R9) at higher $[NO_x]$

Table 5. Initial Conditions of Physical and Thermodynamic Variables Used in the Simulations

Factor	Value
Date	15 Jan.
Latitude	$-45°$
Longitude	$145°$
Height	1000 m
Temperature	291 K (fixed)
Pressure	950 mbar (fixed)
Air density	1.2 kg m^{-3} (fixed)
Water vapor mixing ratio	8.6 g kg^{-1} (fixed)
Liquid water content	variable (0~0.27 g kg^{-1}, see Figure 1)
Droplet radius	variable (0~4.5 μm, see Figure 1)

impedes the buildup of HO_2 and consequently HO_2 decreases as NO_x is increased above 100 ppt. The CH_3O_2 loss is linked to NO_x concentrations through the reaction (R10) and thus CH_3O_2 loss is increased in high NO_x regimes (Figure 2c).

[28] The gaseous source of H_2O_2 in the remote troposphere is the reaction of HO_2 with itself (reaction (R1)). H_2O_2 levels, shown in Figure 2d, thus follow the trends in HO_2, with maxima at intermediate $NO_x \sim 50$ ppt. These results are consistent with those of *Lelieveld and Crutzen* [1991]. They pointed out that if NO_x mixing ratios are below about 100 ppt, the buildup of H_2O_2 is not substantially impeded by competition for HO_2 by NO, so that H_2O_2 mixing ratios may reach up to 1.5 ppbv or more.

[29] Figure 2e shows that CH_3OOH concentrations are inversely proportional to NO_x concentrations. As discussed earlier, $CH_3OOH(g)$ is generated through the reaction (R2) of HO_2 and

CH_3O_2 radicals. The H_2O_2 and CH_3OOH trends combine to produce an increase in the H_2O_2/CH_3OOH ratio with NO_x mixing ratio (Figure 2f); the ratio is insensitive to $[O_3]$. In general, ozone concentrations play an important role in determining the species concentrations only in the unpolluted low NO_x regime. In particular, $[H_2O_2]$ is quite sensitive to $[O_3]$ at low and intermediate $[NO_x]$.

4.2. Results From Cases With Cloud Contact

[30] The species concentrations predicted by the steady state gas phase simulations were used as initial conditions for 4-day time-dependent simulations, with and without cloud contact. In those simulations, $[O_3]$ was again held fixed, and the NO_x source terms described in section 4.1 were applied; dry deposition losses of H_2O_2 and HNO_3 were included. For heterogeneous chemistry the cloud contact history and liquid water content (LWC) history during cloud contact are important. Most prior studies examining heterogeneous chemistry have assumed contact for a finite period of time (usually a few hours) and at constant LWC. Our large eddy simulations (LES) of cloudy boundary layers have shown that air parcels experience a wide variety of trajectories as they pass through cloud [*Stevens et al.*, 1996]. The nature of these trajectories, and the LWC content along these trajectories is a function of the convective nature of the boundary layer and type of cloud cover. In this work, cloud contact was described by a parcel trajectory through cloud, as shown in Figure 1, which depicts the trajectory LWC and droplet radius. We repeated this trajectory six times to allow for extended contact because our existing parcel trajectories only have information on 1 hour's worth of cloud contact. The single trajectory is such that the air parcel spends only about 12 min of each hour inside the cloud; thus for six cycles,
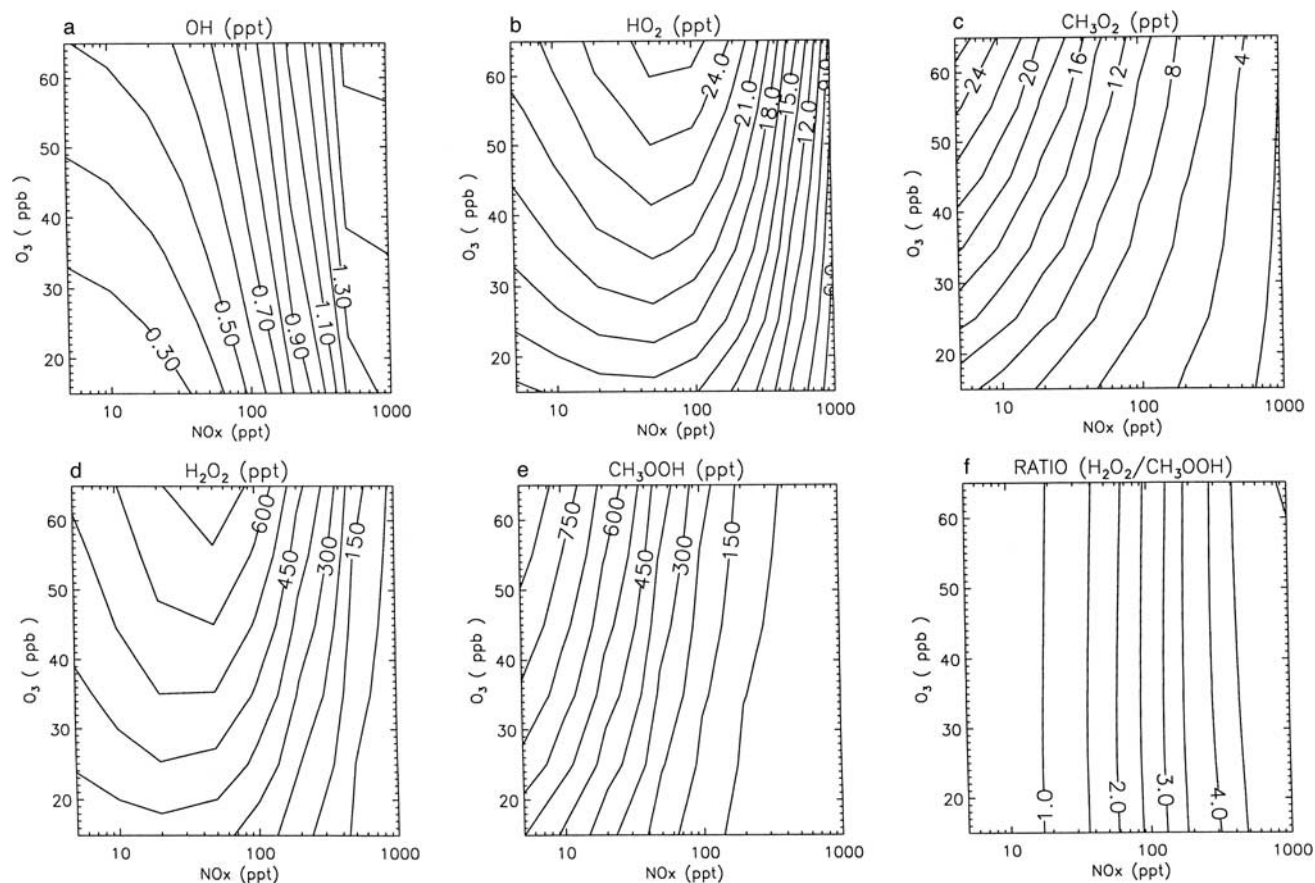

Figure 2. Gas phase concentrations (ppt) predicted by the equilibrium simulation. (a) OH, (b) HO_2 (c) CH_3O_2, (d) H_2O_2, (e) CH_3OOH, and (f) the ratio of H_2O_2/CH_3OOH.

Table 6. Initial Conditions Predicted by Gas Phase Equilibrium Chemistry for Fixed NO_x Concentrations (at Midnight)

Species	Concentrations		
	$NO_x{}^a$ = 5 ppt	$NO_x{}^a$ = 50 ppt	$NO_x{}^a$ = 500 ppt
H_2O_2, ppt	370	409	64.1
CH_3OOH, ppt	663	229	11.7
HNO_3, ppt	4.38	87.4	1710
O_3, ppb (fixed)	25.0	25.0	25.0
NO_y, ppt	10.03	141.6	2242
HCHO, ppt	111	199	329
CO, ppb	49	49	49
CH_4, ppm	1.68	1.68	1.68

[a] NO_x source rates of 0.19, 3.96, and 71.3 ppt h^{-1} were imposed for NO_x = 5, 50, and 500 ppt, respectively.

covering 6 hours of simulation time, the total contact time is 72 min in cloud, broken up into six, 12-min segments. The cloud is nonprecipitating, and no species were permanently removed by wet deposition; the dissolved gases are returned to the gas phase upon cloud evaporation.
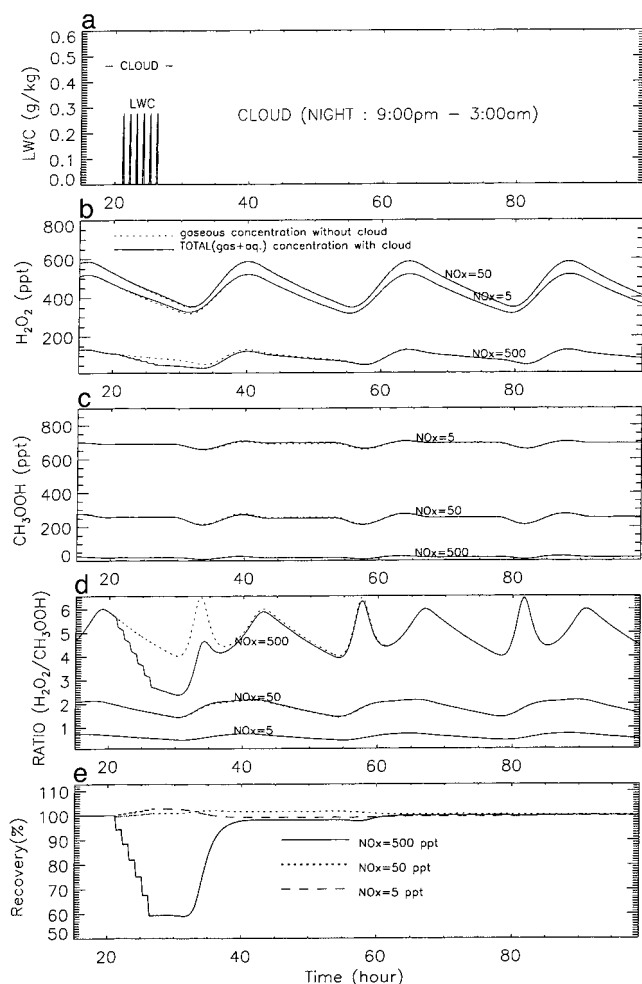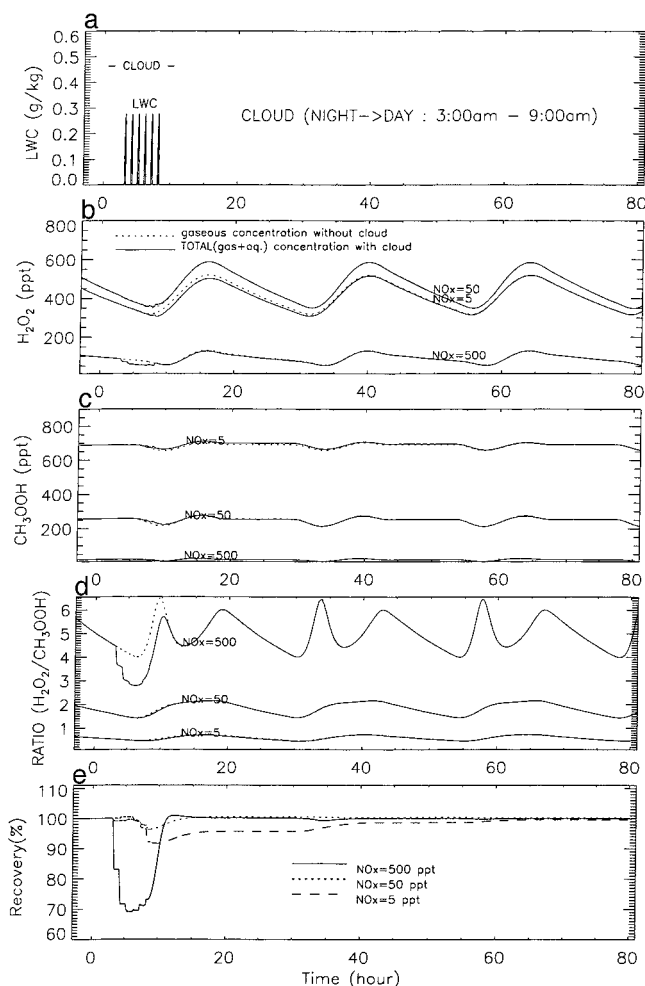

Figure 3. Parcel history for a nighttime cloud encounter. (a) cloud LWC time history. (b and c) Peroxide concentrations as functions of initial [NO_x]. (d) Ratio of hydrogen peroxide to methylhydroperoxide. (e) Comparison of ratio in cloud-processed air with that in a parcel that never encountered cloud, but otherwise had the same history. Abscissa is the hour of the day, where 0, 24,... = midnight.

[31] We show results for three different initial [NO_x], 5, 50, and 500 ppt, and for cloud encounters occurring at different times of the day. To assess the overall effect of the cloud contact on the chemistry, we also ran time-dependent, gas-phase only simulations along the same trajectories for the same three initial conditions; the differences in species concentrations between the paired cloudy and clear cases are examined. A number of sensitivity tests were based on the 50 ppt NO_x case with a daytime cloud encounter, which we will refer to as the "base case." In the first sensitivity test all the aqueous phase N(V) was removed when the cloud droplets were evaporated. This can be regarded as an upper bound on the expected effect of transfer of some $HNO_3(g)$ to particulate nitrate. Second, we examined the role of drop radius by modifying the mean drop size. Third, we considered the sensitivity to dry deposition of gases to the surface. The initial gas-only equilibrium was reestablished under the assumption that no dry deposition losses of H_2O_2 and HNO_3 occurred; the time-dependent cases were rerun from this revised initial condition, also neglecting dry deposition. Fourth, we considered the effects of consumption of H_2O_2 by reaction with $SO_2(g)$. Fifth, we studied the sensitivity of the system to chlorine chemistry. Finally, we repeated the base case with a higher fixed [O_3] to examine the robustness of our conclusions.

[32] The species concentrations predicted by equilibrium chemistry for fixed NO_x concentrations of 5, 50, and 500 ppt were used as inputs to the time-dependent simulation (Table 6). These initial conditions were checked for consistency with observations from PEM-West and MLOPEX [*Singh et al.*, 1996; *Talbot et al.*, 1996; *Brasseur et al.*, 1996]. All the simulations were run for a total of 4 days, but the hour of the day during which cloud was encountered was varied. Figures 3–5 show the simulated peroxide species concentrations for different times of cloud interception of the parcel: nighttime, early morning, and daytime, respectively. As described earlier, the ratio [H_2O_2]/[CH_3OOH] has been used in observations to diagnose cloud processing of air masses, particularly those that have experienced H_2O_2 removal via a precipitation sink. We therefore examined the change in this ratio after the air parcel was released from the nonprecipitating cloud. The predicted ratios prior to cloud contact are consistent with those reported from observations and ranged from <1 for low NO_x conditions to ~1.5–2 for NO_x = 50 ppt, up to ~4.5 –5.5 for high NO_x conditions, with increasing diurnal variations with increasing NO_x levels. We show the cloud effect on the ratio in the lowest panels in Figures 3–5 as the percent recovery of the ratio. This quantity was computed from the difference between the [H_2O_2]/[CH_3OOH] ratio in the cloudy (shown in Figures 3–5) and equivalent clear simulations, expressed as a percentage of the clear-sky ratio.

[33] For the nighttime cloud contact (Figure 3) the presence of cloud has only a minor effect on the peroxide species for low and intermediate [NO_x]. Under higher-NOx conditions ([NO_x] = 500 ppt), however, cloud contact decreases both [H_2O_2] and the ratio, in spite of the fact that there is no permanent precipitation loss.
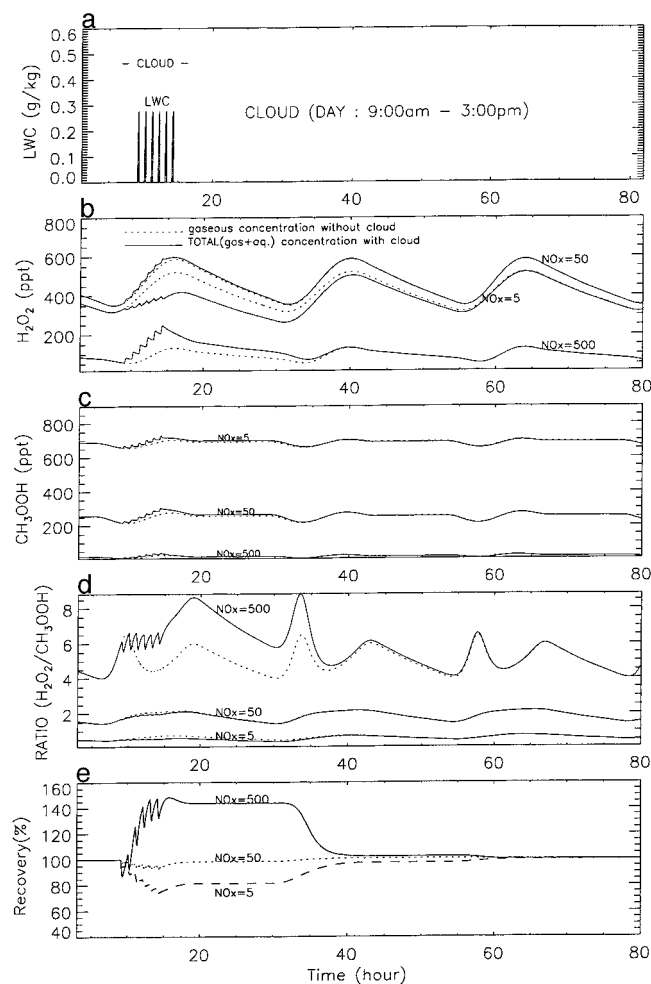
Figure 4.   As in Figure 3, except for the time of cloud encounter.

ous) and the ratio are enhanced by cloud contact for high NO_x conditions. This is in marked contrast to the nighttime cloud case, where the cloud encounter depleted H_2O_2 in the absence of these free-radical peroxide production pathways. The high pH in the low-NO_x cloud favors the aqueous phase production of CH_3OOH via (A35) but hinders H_2O_2 production, and hence the ratio in that case is lowered by cloud contact. Production of both peroxides occurs in the intermediate-NO_x case, with the overall result that the ratio is not strongly perturbed. Photochemical recovery in the daytime cloud simulations is delayed for nearly a full day because the cloud dissipates at 1500 LT.

[35]   Because of the sensitivity of aqueous production of H_2O_2 to pH (A7), we tested the robustness of the results in Figure 5 by fixing pH at values 3.5, 4.5, and 5.8 rather than allowing the model to calculate pH independently. This exercise allowed us to determine the relative importance of NO_x and pH in controlling peroxide chemistry. It was found (results not shown) that at NO_x = 500 ppt the enhancement in H_2O_2, the ratio of H_2O_2/CH_3OOH, as well as the recovery of the ratio to precloud levels were qualitatively similar to those observed in Figure 5. For pH = 3.5 and 4.5 the enhancement in the ratio was still on the order of 40%, and only at pH = 5.8 did the enhancement reduce to 25%. However at low NO_x (5 ppt) the reduction in the ratio of ~20% (relative to no cloud contact) shown in Figure 5 all but disappeared when the pH was fixed at 3.5 and 4.5 but, as expected, remained much the same at pH = 5.8. For 50 ppt, reduction in the ratio of ~10% occured for pH = 5.8 but was virtually unchanged from the result in

There is no aqueous-phase source of H_2O_2 at night, but the loss reaction (A17), involving the dissolved nitrate radical, is active and is most important at higher-NO_x conditions, resulting in a 40% reduction in the ratio from its expected clear-sky value. The depressed ratio persists until sunrise and then recovers over about 6 hours. For the morning cloud (Figure 4), photochemical recovery of the ratio to clear-sky levels is rapid for all NO_x levels.

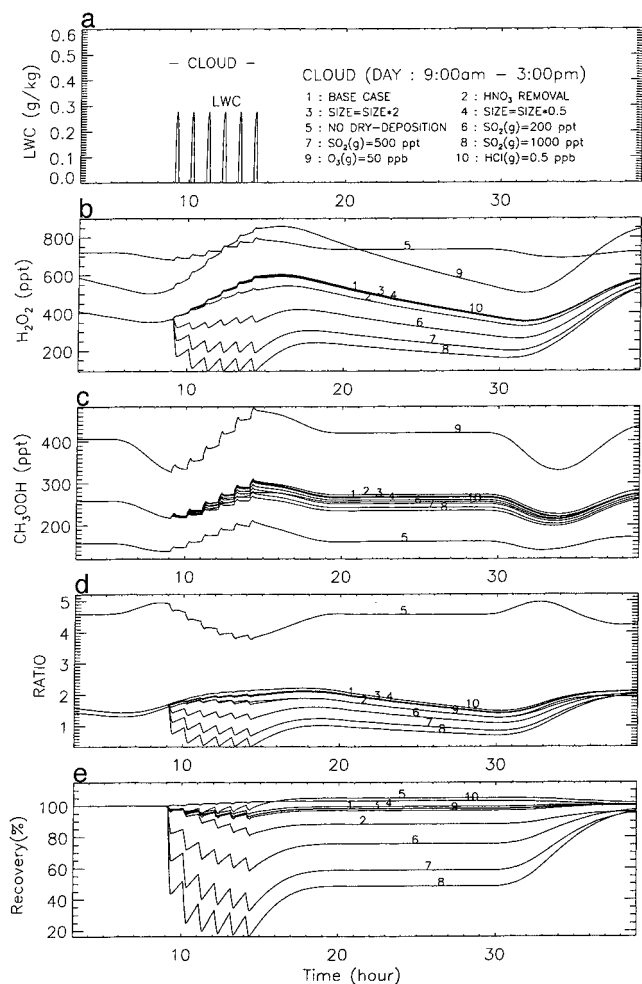[34]   In the daytime cloud contact case (Figure 5) the overall result is an increase in the ratio (~40%) under high-NO_x conditions, a decrease (~20%) for low NO_x conditions, and minimal impact on the ratio at intermediate [NO_x]. The precloud concentrations of $HO_2(g)$ in Figure 2 are 16.5, 18.5, 10.0 ppt for NO_x = 5, 50, 500 ppt, respectively, and because the simulated uptake process is proportional to the gas phase HO_2 concentrations, aqueous phase concentrations of HO_2 (tot)(=O_2^- + HO_2 (aq)) are 0.30, 0.35, and 0.20 ppt for NO_x = 5, 50 and 500 ppt, respectively. However the speciation of HO_2 (tot) in solution is quite different because of differences in computed cloud water pH. The low-NO_x cloud has a pH of ~5.8, whereas the intermediate and high NO_x cases have pHs of ~4.8 and ~3.5. The O_2^- contributions to HO_2 (tot) are 95, 60, and 10% for NO_x = 5, 50, and 500 ppt, respectively. Thus the production of H_2O_2 (aq) through (A7) is most enhanced over the clear-sky rate at intermediate NO_x (50 ppt) where pH is close to optimal. However the small fraction of O_2^- at high NO_x reduces the OH (aq) production through reaction (A13), resulting in a smaller loss of H_2O_2 (aq) via (A5), and higher H_2O_2 (aq) compared with intermediate NO_x conditions. Thus the total H_2O_2 (gas + aque-

Figure 5.   As in Figure 3, except for the time of cloud encounter.

Figure 6. As in Figure 5, except for parcel history in several sensitivity tests. (1) base case for [NO$_x$] = 50 ppt; (2) considering the conversion process of HNO$_3$ to aerosol; (3) doubling the mean size of cloud drops; (4) halving the mean drop size; (5) excluding dry deposition; (6) adding a constant [SO$_2$(g)] = 200 ppt and including S(IV) in-cloud oxidation; (7) and (8) as in case 6 but for 500 and 1000 ppt of SO$_2$(g); (9) setting fixed [O$_3$] = 50 ppb, which is double that in the base case; (10) including chlorine chemistry with [HCl] = 0.5 ppt, Cl$^-$ = 5.6 × 10^{-4}M.

Figure 5 at pH = 3.5 and 4.5. We conclude that pH is an important controlling factor at low to intermediate NO$_x$ but that at high NO$_x$ the enhancement in the ratio observed in Figure 5 is a robust feature.

4.3. Results From Sensitivity Studies

[36] Figure 6 depicts the results of several sensitivity tests for the recovery of the ratio of H$_2$O$_2$ to CH$_3$OOH for the case [NO$_x$] = 50 ppt for the daytime cloud encounter (0900 ∼ 1500 LT). The base case results show that H$_2$O$_2$ levels are ∼350 ppt in clear air before contact with cloud and that cloud contact leads to only a small reduction in the ratio by photochemical reactions involving HO$_x$ radicals. Factor of 2 variations in the sizes of the cloud droplets, as shown in Figure 6 (cases 3 and 4), do not affect the ratio differently than in the base case, even though drop size strongly affects the rate of uptake of gas-phase HO$_2$ and OH on cloud drops [*Frost et al.*, 1999].

[37] An upper bound for the permanent conversion of HNO$_3$(g) to aerosol is considered by removing all cloud water N(V) during each cloud evaporation cycle (case 2). Removal of HNO$_3$ leads to

increases in cloud water pH, and thus this sensitivity test has less in-cloud H$_2$O$_2$ production relative to the base case but slightly more CH$_3$OOH production, resulting in an overall reduction in the ratio of ∼20% immediately after cloud evaporation.

[38] For the case where dry deposition was neglected (case 5), the gas phase model shows that the initial steady state H$_2$O$_2$ and HNO$_3$ gas phase concentrations are significantly increased over those in the base case. In contrast, [RO$_x$] (RO$_x$ = OH + HO$_2$ + CH$_3$O$_2$) and [HO$_2$] are not directly affected by dry deposition, and thus the H$_2$O$_2$ production rate via (R1) is also maintained. Therefore the main reason for the lower initial H$_2$O$_2$ levels in clear air in the base case is the H$_2$O$_2$ dry deposition sink itself, and not any chemical feedbacks. Although [RO$_x$] is nearly unchanged, [OH] is increased, and [CH$_3$O$_2$] is decreased relative to values in the base case. The lower [CH$_3$O$_2$] leads to decreases in CH$_3$OOH (Figure 6c), leading in turn to significantly higher values of the ratio. The recovery process is very similar to the cases with dry deposition since the main production of H$_2$O$_2$ through reaction (R1) is not influenced much.

[39] Sensitivity cases 6−8 include SO$_2$(g) and its aqueous-phase reactions (Table 7) in the simulations. Dissolved S(IV) will react with both H$_2$O$_2$(aq) and O$_3$(aq); the rate of the reaction with O$_3$ is strongly pH dependent. We did not simulate any gas-phase S chemistry but instead kept [SO$_2$(g)] constant during the 4-day time-dependent simulations as an upper bound on its effects. The base case had maximum pH values (near the maximum LWC) of ∼4.8, whereas the pH dropped to ∼4 and ∼3.8, respectively, in the first and final cloud encounters in the SO$_2$(g) = 200 ppt case including S(IV) oxidation to S(VI); both pH levels are reasonable for remote, relatively clean clouds. Results (Figure 6) indicate that the permanent consumption of H$_2$O$_2$ by S oxidation reactions has a noticeable effect (−40%) on postcloud levels of H$_2$O$_2$. We also ran cases for [SO$_2$(g)] = 500 and 1000 ppt. The pH dropped to lower values in those cases (∼4.3−3.5), and the higher S(IV) concentrations effectively consumed H$_2$O$_2$. As a result, the [H$_2$O$_2$] was more strongly modified in those cases, up to a factor of 5 for [SO$_2$(g)] = 1000 ppt. The ratios [H$_2$O$_2$]/[CH$_3$OOH] were therefore also significantly lowered by cloud contact, but recovery rates in all cases were similar, requiring a diurnal cycle to reestablish clear-sky values.

[40] In sensitivity case 9 the fixed ozone concentration was increased to 50 ppb. As might be deduced from Figure 2, and as seen in Figure 6, the gas-phase steady state concentrations of H$_2$O$_2$ and CH$_3$OOH were increased; but the initial value of the ratio, and its recovery behavior after cloud contact, were very similar to those in the base case. Thus the choice of fixed ozone concentration should not have a large effect on the simulated species timelines, except for those cases in which S(IV) oxidation is considered.

[41] In sensitivity case 10, chlorine chemistry was included (Table 7) and HCl(g) = 0.5 ppb, Cl$^-$ = 5.6 × 10^{-4}M were used as initial conditions [*Herrmann et al.*, 1999]. The chlorine chemistry increases the concentration of HO$_2$ (tot)(∼10%) but decreases O$_2^-$ due to the lower pH (∼4.0), and thus in-cloud production of H$_2$O$_2$ via (A7) is little affected. Therefore the recovery rate after cloud contact looks very similar to that in the base case.

5. Summary and Conclusions

[42] We have applied a coupled gas and aqueous phase chemical/microphysical model to study the effect of a nonprecipitating marine stratocumulus cloud on gas-phase H$_2$O$_2$, CH$_3$OOH, and the ratio H$_2$O$_2$/CH$_3$OOH. In clear air the ratio of these two species is expected to vary with [NO$_x$] because of their photochemical sources. Differences in the solubility of H$_2$O$_2$ and CH$_3$OOH have been used in prior studies to argue that variations in the ratio are also indicators of recent precipitation removal of H$_2$O$_2$. We investigated the variation in clear-sky levels of H$_2$O$_2$/CH$_3$OOH as functions of [O$_3$] and [NO$_x$], the perturbations induced by contact with nonprecipitating cloud, and the rate at which this ratio recovers to clear-sky levels after the parcel is released from cloud into clear air. Steady

Table 7. Chlorine and Sulfur Chemistry for Sensitivity Test

	K_{298}, M or M atm^{-1}	$-\Delta H/R$, K	Reference
Henry's Law Constants			
(H15) HCl	7.27(2)	2020	*Marsh and McElroy* [1985]
(H16) SO_2	1.23(0)	3120	*Smith and Martell* [1976]
Aqueous Phase Equilibrium Reactions			
(E9) $HCl(aq) \leftrightarrows H^+ + Cl^-$	1.74(6)	6900	*Marsh and McElroy* [1985]
(E10) $Cl_2^- \leftrightarrows Cl + Cl^-$	5.26(−6)		*Jayson et al.* [1973]
(E11) $SO_2(aq) \leftrightarrows HSO_3^- + H^+$	1.23(−2)	1960	*Smith and Martell* [1976]
(E12) $HSO_3^- \leftrightarrows SO_3^{2-} + H^+$	6.61(−8)	1500	*Smith and Martell* [1976]
(E13) $H_2SO_4(aq) \leftrightarrows HSO_4^- + H^+$	1.0(3)		*Perrin* [1982]
(E14) $HSO_4^- \leftrightarrows SO_4^- + H^+$	1.02(−2)	2720	*Smith and Martell* [1976]
Chlorine Chemistry			
(A39) $Cl^- + OH \longrightarrow ClOH^-$	4.3(9)	−1500	*Jayson et al.* [1973]
(A40) $ClOH^- \longrightarrow Cl^- + OH$	6.1(9)		*Jayson et al.* [1973]
(A41) $ClOH^- \xrightarrow{H+} Cl + H_2O$	2.1(10)×[H$^+$]		*Jayson et al.* [1973]
(A42) $Cl \xrightarrow{H_2O} ClOH^- + H^+$	1.3(3)		*Jayson et al.* [1973]
(A43) $HO_2 + Cl_2^- \longrightarrow 2\,Cl^- + O_2 + H^+$	4.5(9)	−1500	*Ross and Neta* [1979]
(A44) $O_2^- + Cl_2^- \longrightarrow 2\,Cl^- + O_2$	1.0(9)	−1500	*Ross and Neta* [1979]
(A45) $HO_2 + Cl \longrightarrow Cl^- + O_2 + H^+$	3.1(9)	−1500	*Graedel and Goldberg* [1983]
(A46) $H_2O_2 + Cl_2^- \longrightarrow 2\,Cl^- + HO_2 + H^+$	1.4(5)	−3370	*Hagesawa and Neta* [1978]
(A47) $H_2O_2 + Cl \longrightarrow Cl^- + HO_2 + H^+$	4.5(7)		*Graedel and Goldberg* [1983]
(A48) $OH^- + Cl_2^- \longrightarrow 2\,Cl^- + OH$	7.3(6)	−2160	*Hagesawa and Neta* [1978]
Sulfur Chemistry			
(A49) $S(IV) \longrightarrow S(VI) + O_2$	2.4(4)		
	3.7(5)	−5530	
	1.5(9)	−5280	*Hoffmann and Calvert* [1985]
(A50) $S(IV) + H_2O_2 \longrightarrow S(VI) + H_2O$	1.3(6)	−4430	*McArdle and Hoffmann* [1983]
(A51) $SO_3^- + OH \xrightarrow{O_2} SO_5^- + OH^-$	4.6(9)	−1500	*Huie and Neta* [1987]
(A52) $HSO_3^- + OH \xrightarrow{O_2} SO_5^- + H_2O$	4.2(9)	−1500	*Huie and Neta* [1987]
(A53) $SO_5^- + HSO_3^- \xrightarrow{O_2} HSO_5^- + SO_5^-$	3.0(5)	−3100	*Huie and Neta* [1987]
$\quad SO_5^- + SO_3^{2-} \xrightarrow{O_2} HSO_5^- + SO_5^-$	1.3(7)	−2000	*Huie and Neta* [1987]
(A54) $SO_5^- + O_2^- \xrightarrow{H_2O} HSO_5^- + CO_2 + HO_2$	1.0(8)	−1500	*Jacob* [1986]
(A55) $SO_5^- + HCOOH \xrightarrow{O_2} HSO_5^- + CO_2 + HO_2$	2.0(2)	−5300	*Jacob* [1986]
(A56) $SO_5^- + HCOO^- \xrightarrow{O_2} HSO_5^- + CO_2 + O_2^-$	1.4(4)	−4000	*Jacob* [1986]
(A57) $SO_5^- + SO_5^- \longrightarrow 2SO_4^- + O_2$	2.0(8)	−1500	*Jacob* [1986]
(A58) $HSO_5^- + HSO_3^- \xrightarrow{H+} 2SO_4^- + 3H^+$	7.5(7)	−4750	*Jacob* [1986]
(A59) $HSO_5^- + OH \longrightarrow SO_5^- + H_2O$	1.7(7)	−1900	*Jacob* [1986]
(A60) $HSO_5^- + SO_4^- \longrightarrow SO_5^- + SO_4^{2-} + H^+$	<1.0(5)		*Jacob* [1986]
(A61) $HSO_5^- + NO_2^- \longrightarrow HSO_4^- + NO_3^-$	3.1(−1)	−6650	*Jacob* [1986]
(A62) $HSO_5^- + Cl^- \longrightarrow SO_4^{2-} + \text{products}$	1.8(−3)	−7050	*Jacob* [1986]
(A63) $SO_4^- + HSO_3^- \xrightarrow{O_2} SO_4^{2-} + H^+ + SO_5^-$	1.3(9)	−1500	*Jacob* [1986]
(A64) $SO_4^- + SO_3^{2-} \xrightarrow{O_2} SO_4^{2-} + SO_5^-$	5.3(8)	−1500	*Jacob* [1986]
(A65) $SO_4^- + HO_2 \longrightarrow SO_4^{2-} + H^+ + O_2$	5.0(9)	−1500	*Jacob* [1986]
(A66) $SO_4^- + O_2^- \longrightarrow SO_4^{2-} + O_2$	5.0(9)	−1500	*Jacob* [1986]
(A67) $SO_4^- + OH^- \longrightarrow SO_4^{2-} + OH$	8.0(7)	−1500	*Jacob* [1986]
(A68) $SO_4^- + H_2O_2 \longrightarrow SO_4^{2-} + H^+ + HO_2$	1.2(7)	−2000	*Ross and Neta* [1979]
(A69) $SO_4^- + NO_2^- \longrightarrow SO_4^{2-} + NO_2$	8.8(8)	−1500	*Jacob* [1986]
(A70) $SO_4^- + HCO_3^- \longrightarrow SO_4^{2-} + H^+ + CO_3$	9.1(6)	−2100	*Ross and Neta* [1979]
(A71) $SO_4^- + HCOO^- \xrightarrow{O_2} SO_4^{2-} + CO_2 + HO_2$	1.7(8)	−1500	*Jacob* [1986]
(A72) $SO_4^- + Cl^- \longrightarrow SO_4^{2-} + Cl$	2.0(8)	−1500	*Ross and Neta* [1979]
(A73) $SO_4^- + HCOOH \xrightarrow{O_2} SO_4^{2-} + H^+ + CO_2 + HO_2$	1.4(6)	−2700	*Jacob* [1986]
(A74) $HSO_3^- + CH_3OOH \longrightarrow SO_4^{2-} + 2\,H^+ + \text{products}$	1.9(7)	−3800	*Hoffmann and Calvert* [1985]
(A75) $S(IV) + HO_2 \longrightarrow S(VI) + OH$	1.0(6)		*Hoffmann and Calvert* [1985]
$\quad S(IV) + O_2^- \xrightarrow{H_2O} S(VI) + OH + OH^-$	1.0(5)		*Hoffmann and Calvert* [1985]
(A76) $SO_4^- + CH_3OH \xrightarrow{O_2} SO_4^{2-} + HCHO + H^+ + HO_2$	2.5(7)	−1800	*Dogliotti and Hayon* [1967]
(A77) $2HSO_3^- + NO_3 \xrightarrow{O_2} NO_3^- + 2\,H^+ + SO_4^{2-} + SO_4^-$	1.0(8)		*Chameides* [1984]
(A78) $2\,NO_2 + HSO_3^- \xrightarrow{H_2O} SO_4^{2-} + 3\,H^+ + 2\,NO_2^-$	2.0(6)		*Lee and Schwartz* [1983]
(A79A)[a] $S(IV) + N(III) \longrightarrow S(VI) + \text{products}$	1.4(2)		*Martin* [1984]
(A79B)[b] $2HSO_3^- + NO_2^- \longrightarrow OH^- + \text{products}$	4.8(3)	−6100	*Oblath et al.* [1981]
(A80) $HCHO + HSO_3^- \longrightarrow HOCH_2SO_3^-$	2.9(2)	−4900	*Boyce and Hoffmann* [1984]
$\quad HCHO + HSO_3^{2-} \xrightarrow{H_2O} HOCH_2SO_3^- + OH^-$	2.5(7)	−1800	*Boyce and Hoffmann* [1984]
(A81) $HOCH_2SO_3^- + OH^- \longrightarrow SO_3^{2-} + HCHO + H_2O$	3.6(3)	−4500	*Munger et al.* [1986]
(A82) $HOCH_2SO_3^- + OH \xrightarrow{O_2} SO_5^- + HCHO + H_2O$	1.4(9)	−1500	*Jacob* [1986]
(A83) $HSO_3^- + Cl_2^- \xrightarrow{O_2} SO_5^- + 2Cl^- + H^+$	3.4(8)	−1500	*Huie and Neta* [1987]
$\quad SO_3^{2-} + Cl_2^- \xrightarrow{O_2} SO_5^- + 2Cl^-$	1.6(8)	−1500	*Huie and Neta* [1987]

[a] For pH ≤ 3.
[b] For pH >3.

state clear-sky values of the ratio increase strongly with increases in $[NO_x]$ but are independent of $[O_3]$. The model simulations showed that even in the absence of precipitation, cloud contact can, under certain conditions, have a pronounced and persistent effect on the ratio. Recovery of the ratio to clear-sky levels is driven by photochemistry, and is thus sensitive to the time of the cloud encounter. If cloud contact and corresponding reductions in the ratio occur in the late afternoon or at night, photochemistry is inactive, and the ratios remain low until well into the next diurnal cycle. When cloud contact occurs at night and is followed soon after by daytime photochemical activity, there is a significant reduction in the ratio only for the high-NO_x conditions.

[43] We tested the sensitivity of our results and conclusions to several assumptions made in the modeling approach. Variations in the droplet size had little effect. Although the modeled ratios themselves were sensitive to the treatment of dry deposition of H_2O_2 and HNO_3, the relative recovery rates of the ratios were not. We assumed in the base case that dissolved $HNO_3(g)$ was returned to the gas phase when the cloud evaporated. Since some nitrate can be retained in the particle phase, we tested this assumption by removing all dissolved HNO_3; the postcloud ratio was reduced by about 20% compared with that in the base case, although the impact could be larger for higher levels of $HNO_3(g)$ than those we used here. It is known that oxidation of S(IV) can be an important sink of H_2O_2. We added the relevant oxidation reactions to the base case, assuming a representative $SO_2(g)$ concentration for clean marine regions of 200 ppt and found that the oxidation reduced cloud pH from ~ 4.8 to ~ 4, with a 40% reduction in both $[H_2O_2]$ and the ratio postcloud. Addition of Cl chemistry to the mechanism did not significantly alter the conclusions for the base case, for the concentrations of Cl species that were simulated. Finally, in this study the chemistry of trace metal ions was not considered. When trace metals are present, in-cloud reactions of dissolved HO_2 and copper dramatically reduce $HO_2(tot)$ and other free radical concentrations [*Walcek et al.*, 1997], which would result in lower values of H_2O_2 and the H_2O_2/CH_3OOH ratio. Reactions with iron may also affect aqueous-phase photochemistry. Measurements of these important trace metal ions that could be used to initialize simulations to examine their effects are needed.

[44] Our results imply that H_2O_2 and CH_3OOH are affected not only by dry and wet deposition losses, as noted in previous studies, but also by interactions with nonprecipitating clouds, even in the presence of negligible $[SO_2(g)]$. The residual effects of the cloud contact are short-lived if the contact occurs early in the day because photochemical processes act quickly to restore photochemical equilibrium, while if cloud contact occurs during the late afternoon or evening, photochemical recovery is hindered. Because of this sensitivity to the time of cloud contact, as well as the uncertainties in the photochemical history of cloud parcels, it may be difficult to use the measurement of the ratio of H_2O_2/CH_3OOH as a general indicator of cloud contact in the interpretation of field data. Nevertheless, it may still be a useful interpretative tool under certain conditions.

References

Anbar, M., and P. Neta, A compilation of specific bimolecular rate constants for the reactions of hydrated electrons, hydrogen atoms and hydroxyl radicals with inorganic and organic compounds in aqueous solution, *Int. J. Appl. Radiat. Isot.*, *18*, 493–523, 1967.

Behar, D., G. Czapski, and I. Duchovny, Carbonate radical in flash photolysis and pulse radiolysis of aqueous carbonate solutions, *J. Phys. Chem.*, *74*, 2206–2210, 1970.

Bielski, B. H. J., Reevaluation of the spectral and kinetic properties of HO_2 and O_2^- free radicals, *Photochem. Photobiol.*, *28*, 645–649, 1978.

Bothe, E., and D. Schulte-Frohlinde, Reaction of dihydroxymethyl radical with molecular oxygen in aqueous solution, *Z. Naturforsch. B Anorg. Chem. Org. Chem.*, *35*, 1035–1039, 1980.

Bower, K. N., and T. W. Choularton, Cloud processing of the cloud condensation nucleus spectrum and its climatological consequences, *Q. J. R. Meteorol. Soc.*, *119*, 655–679, 1993.

Boyce, S. D., and M. R. Hoffmann, Kinetics and mechanism of the formation of hydroxymethanesulfonic acid at low pH, *J. Phys. Chem.*, *88*, 4740–4746, 1984.

Brasseur, G. P., D. A. Hauglustaine, and S. Walters, Chemical compounds in the remote Pacific troposphere: Comparison between MLOPEX measurements and chemical transport model calculations, *J. Geophys. Res.*, *101*, 14,795–14,813, 1996.

Chameides, W. L., The photochemistry of a remote marine stratiform cloud, *J. Geophys. Res.*, *89*, 4739–4755, 1984.

Chen, S., V. W. Cope, and M. Z. Hoffman, Behavior of CO_3 radicals generated in the flash photolysis of carbonatoamines complexes of cobalt(III) in aqueous solution, *J. Phys. Chem.*, *77*, 1111–1116, 1973.

Christensen, H., K. Sehested, and H. Corfitzen, Reactions of hydroxyl radicals with hydrogen peroxide at ambient and elevated temperatures, *J. Phys. Chem.*, *86*, 1588–1590, 1982.

Cohan, D. S., M. G. Schultz, D. J. Jacob, B. G. Heikes, and D. R. Blake, Convective injection and photochemical decay of peroxides in the tropical troposphere: Methyl iodide as a tracer of marine convection, *J. Geophys. Res.*, *104*, 5717–5724, 1999.

Dahlback, A., and K. Stamnes, A new spherical model for computing the radiation field available for photolysis and heating at twilight, *Planet. Space Sci.*, *39*, 671–683, 1991.

Daum, P. H., L. I. Kleinman, A. J. Hills, A. L. Lazrus, A. C. D. Leslie, K. Busness, and J. Boatman, Measurement and interpretation of concentrations of H_2O_2 and related species in the upper Midwest during summer, *J. Geophys. Res.*, *95*, 9857–9871, 1990.

Davis, D. D., et al., Assessment of ozone photochemistry in the western North Pacific as inferred from PEM-West A observations during the fall 1991, *J. Geophys. Res.*, *101*, 2111–2134, 1996.

DeMore, W. B., S. P. Sander, D. M. Golden, R. F. Hampson, M. J. Kurylo, C. J. Howard, A. R. Ravishankara, C. E. Kolb, and M. J. Molina, Chemical kinetics and photochemical data for use in stratospheric modeling, Evaluation number 12, *JPL Publ., 97-4*, 1997.

Dogliotti, L., and E. Hayon, Flash photolysis of persulfate ions in aqueous solutions: Study of the sulfate and ozonide radical ions, *J. Phys. Chem.*, *71*, 2511–2516, 1967.

Feingold, G., and S. M. Kreidenweis, Does cloud processing of aerosol enhance droplet concentrations?, *J. Geophys. Res.*, *105*, 24,351–24,362, 2000.

Feingold, G., S. M. Kreidenweis, and Y. Zhang, Statocumulus processing of gases and cloud condensation nuclei, 1, Trajectory ensemble model, *J. Geophys. Res.*, *103*, 19,527–19,542, 1998.

Frost, G. J., et al., Photochemical modeling of OH levels during the First Aerosol Characterization Experiment (ACE 1), *J. Geophys. Res.*, *104*, 16,041–16,052, 1999.

Fuchs, N. A., and A. G. Sutugin, High-dispersed aerosols, *Int. Rev. Aerosol Phys. Chem.*, *2*, 1–60, 1971.

Gardner, J. A., L. R. Watson, Y. G. Adewuyi, P. Davidovits, M. S. Zahniser, D. R. Worsnop, and C. E. Kolb, Measurement of the mass accomodation coefficient of $SO_2(g)$ on water droplets, *J. Geophys. Res.*, *92*, 10,887–10,895, 1987.

Graedel, T. E., and K. I. Goldberg, Kinetic studies of raindrop chemistry, 1, Inorganic and organic processes, *J. Geophys. Res.*, *88*, 10,865–10,882, 1983.

Graedel, T. E., and C. J. Weschler, Chemistry within aqueous atmospheric aerosols and raindrops, *Rev. Geophys.*, *19*, 505–539, 1981.

Hagesawa, K., and P. Neta, Rate constants and mechanisms of reaction for Cl_2^- radicals, *J. Phys. Chem.*, *82*, 854–857, 1978.

Hegg, D. A., The relative importance of major aqueous sulfate formation reactions in the atmosphere, *Atmos. Res.*, *22*, 323–333, 1989.

Hegg, D. A., R. Majeed, P. F. Yuen, M. B. Baker, and T. V. Larson, The impacts of SO_2 oxidation in cloud drops and in haze particles on aerosol light scattering and CCN activity, *Geophys. Res. Lett.*, *23*, 2613–2616, 1996.

Heikes, B., Formaldehyde and hydroperoxides at Mauna Loa Observatory, *J. Geophys. Res.*, *97*, 18,001–18,014, 1992.

Heikes, B. G., et al., Hydrogen peroxide and methylhydroperoxide distributions related to ozone and odd oxygen over the North Pacific in the fall of 1991, *J. Geophys. Res.*, *101*, 1891–1905, 1996.

Herrmann, H., B. Ervens, P. Nowacki, R. Wolke, and R. Zellner, A chemical aqueous phase radical mechanism for tropospheric chemistry, *Chemosphere*, *38*, 1123–1232, 1999.

Herrmann, H., B. Ervens, H.-W. Jacobi, R. Wolke, P. Nowacki, and R. Zellner, CAPRAM2.3: A chemical aqueous phase radical mechanism for tropospheric chemistry, *J. Atmos. Chem.*, *36*, 231–284, 2000.

Hoffmann, M. R., and J. G. Calvert, Chemical transformation modules for eulerian acid deposition models, vol. 2, The aqueous-phase chemistry, *EPA/600/3-85/017*, U.S. Environ. Prot. Agency, Research Triangle Park, N. C., 1985.

Hoigne, J., and H. Bader, Rate constants of reactions of ozone with organic and inorganic compounds in water, 1, Non-dissociating orgnic compounds, *Water Res.*, 17, 173–183, 1983a.

Hoigne, J., and H. Bader, Rate constants of reactions of ozone with organic and inorganic compounds in water, 2, Dissociating organic orgnic compounds, *Water Res.*, 17, 185–194, 1983b.

Huie, R. E., and P. Neta, Rate constants for some oxidations of S(IV) by radicals in aqueous solutions, *Atmos. Environ.*, 21, 1743–1747, 1987.

Jacob, D. J., Chemistry of OH in remote clouds and its role in the production of formic acid and peroxymonosulfate, *J. Geophys. Res.*, 91, 9807–9826, 1986.

Jacob, P., and D. Klockow, Hydrogen peroxide measurements in the marine atmosphere, *J. Atmos. Chem.*, 15, 353–360, 1992.

Jacob, P., T. M. Tavares, V. C. Rocha, and D. Klockow, Atmospheric H_2O_2 field measurements in a tropical environment: Bahia, Brazil, *Atmos. Environ., Part A*, 24, 377–382, 1990.

Jayson, G. G., B. J. Parsons, and A. J. Swallow, Some simple, highly reactive, inorganic chlorine derivatives in aqueous-solution, *Trans. Faraday Soc.*, 69, 1597–1607, 1973.

Kozac-Channing, L. F., and G. R. Heltz, Solubility of ozone in aqueous solutions of $0\sim0.6$ M ionic strength at $5\sim30C$, *Environ. Sci. Technol.*, 17, 145–149, 1983.

Kunen, S. M., A. L. Lazrus, G. L. Kok, and B. G. Heikes, Aqueous oxidation of SO_2 by hydrogen peroxide, *J. Geophys. Res.*, 88, 3671–3674, 1983.

Latimer, W. M., *The Oxidation States of the Elements and Their Potentials in Aqueous Solutions*, pp. 70–89, Prentice-Hall, New York, 1952.

Ledbury, W., and E. W. Blair, The partial formaldehyde vapour pressure of aqueous solutions of formaldehyde, II, *J. Chem. Soc.*, 127, 2832–2839, 1925.

Lee, Y.-N., and S. E. Scwartz, Kinetics of oxidation of aqueous sulfur(IV) by nitrogen dioxide, in *Precipitation Scavenging, Dry Deposition, and Resuspension*, vol. 1, edited by H. R. Pruppacher, R. G. Semonin and W. G. N. Slinn, Elsevier Sci., New York, 1983.

Le Henaff, P., Methodes d'etude et proprietes des hydrates, hemiacetals et hemiacetals derives des aldehydes et des cetones, *Bull. Soc. Chim. France*, 4687–4700, 1968.

Lelieveld, J., and P. J. Crutzen, The role of clouds in tropospheric photochemistry, *J. Atmos. Chem.*, 12, 229–267, 1991.

Lind, J. A., and G. L. Kok, Henry's law determinations for aqueous solutions of hydrogen peroxide, methylhydroperoxide, and peroxyacetic acid, *J. Geophys. Res.*, 91, 7889–7895, 1986.

Liu, S. C., et al., A study of the photochemistry and ozone budget during the Mauna Loa Observatory Photochemistry Experiment, *J. Geophys. Res.*, 97, 10,463–10,471, 1992.

Logan, J. A., M. J. Prather, S. C. Wofsy, and M. B. McElory, Tropospheric chemistry: A global perspective, *J. Geophys. Res.*, 86, 7210–7254, 1981.

Maahs, H. G., Kinetics and mechanism of the oxidation of S(IV) by ozone in aqueous solution with particular reference to SO_2 conversion in nonurban tropospheric clouds, *J. Geophys. Res.*, 88, 10,721–10,732, 1983.

Macdonald, A. M., K. G. Anlauf, C. M. Banic, W. R. Leaitch, and H. A. Wiebe, Airborne measurements of aqueous and gaseous hydrogen peroxide during spring and summer in Ontario, Canada, *J. Geophys. Res.*, 100, 7253–7262, 1995.

Marsh, A. R. W., and W. J. McElroy, The dissociation constants and Henry's law constant of HCl in aqueous solution, *Atmos. Environ.*, 19, 1075–1080, 1985.

Martell, A. E., and R. M. Smith, *Critical Stability Constants*, vol. 3, *Other Organic Ligands*, Plenum, New York, 1977.

Martin, D., M. Tsivou, B. Bonsang, C. Abonnel, T. Carsey, M. Springer-Young, A. Pszenny, and K. Suhre, Hydrogen peroxide in the marine atmospheric boundary layer during the Atlantic Stratocumulus Transition Experiment/Marine Aerosol and Gas Exchange Experiment in the eastern subtropical North Atlantic, *J. Geophys. Res.*, 102, 6003–6016, 1997.

Martin, L. R., *Kinetic Studies of Sulfite Oxidation in Aqueous Solution in SO_2, NO and NO_2 Oxidation Mechanisms: Atmospheric Considerations*, edited by J. G. Calvert, pp. 63–100, Butterworth-Heinemann, Woburn, Mass., 1984.

Martin, L. R., and D. E. Damschen, Aqueous oxidation of sulfur dioxide by hydrogen peroxide at low pH, *Atmos. Environ.*, 15, 1615–1622, 1981.

McArdle, J. V., and M. R. Hoffmann, Kinetics and mechanism of the oxidation of aquated sulfur dioxide by hydrogen peroxide at low pH, *J. Phys. Chem.*, 87, 5425–5429, 1983.

McElroy, W. J., Sources of hydrogen peroxides in cloudwater, *Atmos. Environ.*, 20, 427–438, 1986.

McKeen, S. A., et al., Photochemical modeling of hydroxyl and its relation-ship to other species during the Tropospheric OH Photochemistry Experiment, *J. Geophys. Res.*, 102, 6467–6493, 1997.

Munger, J. W., C. Tiller, and M. R. Hoffmann, Indentification of hydro-xymethanesulfonate in fog water, *Science*, 231, 247–249, 1986.

Oblath, S. B., S. S. Markowitz, T. Novakov, and S. G. Chang, Kinetics of the formation of hydroxylamine disulfonate by reaction of nitrate with sulfites, *J. Phys. Chem.*, 85, 1017–1021, 1981.

O'Sullivan, D. W., B. G. Heikes, M. Lee, W. Chang, G. L. Gregory, D. R. Blake, and G. W. Sachse, Distribution of hydrogen peroxide and methyl-hydroperoxide over the Pacific and South Atlantic Oceans, *J. Geophys. Res.*, 104, 5635–5646, 1999.

Pandis, S., and J. H. Seinfeld, Sensitivity analysis of a chemical mechanism for aqueous-phase atmospheric chemistry, *J. Geophys. Res.*, 94, 1105–1126, 1989.

Penkett, S. A., B. M. R. Jones, K. A. Brice, and A. E. Eggleton, The importance of atmospheric ozone and hydrogen peroxide in oxidizing sulphur dioxide in cloud and rainwater, *Atmos. Environ.*, 13, 123–137, 1979.

Perrin, D. D., *Inoization Constants of Inorganic Acids and Bases in Aqueous Solution,* 2nd ed., Pergamon, New York, 1982.

Price, C., J. Penner, and M. Prather, NO_x from lightning, 1, Global distribution based on lightning physics, *J. Geophys. Res.*, 102, 5929–5941, 1997.

Ravishankara, A. R., Heterogeneous and multiphase chemistry in the troposphere, *Science*, 276, 1058–1065, 1997.

Ross, A. B., and P. Neta, Rate constants for reactions of inorganic radicals in aqueous solution, *Rep. NSRDS-NBS 65*, Natl. Bur. of Stand., U.S. Dep. of Commer., Washington, D. C., 1979.

Schmidt, K. H., Electrical conductivity techniques for studying the kinetics of radiation-induced chemical reactions in aqueous solutions, *Int. J. Radiat. Phys. Chem.*, 4, 439–468, 1972.

Scholes, G., and R. L. Willson, γ-radiolysis of aqueous thymine solutions: Determination of relative reaction rates of OH radicals, *Trans. Faraday Soc.*, 63, 2982–2993, 1967.

Schwartz, S. E., Gas- and aqueous-phase chemistry of HO_2 in liquid water clouds, *J. Geophys. Res.*, 89, 11,589–11,598, 1984.

Schwartz, S. E., Mass-transport considerations pertinent to aqueous-phase reactions of gases in liquid-water clouds, in *Chemistry of Multiphase Atmospheric Systems*, edited by W. Jaeschke, pp. 415–471, Springer-Verlag, New York, 1986.

Schwartz, S. E., and W. H. White, Solubility equilibrium of the nitrogen oxides and oxyacids in dilute aqueous solution, *Adv. Environ. Sci. Eng.*, 4, 1–45, 1981.

Sehested, K., O. Rasmussen, and H. Fricke, Rate consatants of OH with Ho_2, O_2^-, and H_2O_2 from hydrogen peroxide formation in pulse-irradiated oxygenated water, *J. Phys. Chem.*, 72, 626–631, 1968.

Sehested, K., J. Holcman, E. Bjergbakke, and E. J. Hart, A pulse radiolytic study of the reaction OH + O_3 in aqueous medium, *J. Phys. Chem.*, 88, 4144–4147, 1984.

Seinfeld, J. H., and S. N. Pandis, *Atmospheric Chemistry and Physics: From Air Pollution to Climate Change*, pp. 596–607, John Wiley, New York, 1998.

Shapilov, O. D., and Y. L. Kostyukovskii, Reaction kinetics of hydrogen peroxide with formic acid in aqueous solutions, *Kinet. Katal.*, 15, 1065–1067, 1974.

Singh, H. B., et al., Reactive nitrogen and ozone over the western Pacific: Distributioin, partitioning, and source, *J. Geophys. Res.*, 101, 1793–1808, 1996.

Smith, R. M., and A. E. Martell, *Critical Stability Constants,* vol. 4, *Inorganic Complexes*, Plenum, New York, 1976.

Staehelin, J., and J. Hoigne, Decomposition of ozone in water: Rate of initiation by hydroxide ions and hydrogen peroxide, *Environ. Sci. Technol.*, 16, 676–681, 1982.

Staffelbach, T. A., G. L. Kok, B. G. Heikes, B. McCully, G. I. Mackay, D. R. Karecki, and H. I. Schiff, Comparison of hydroperoxide measurements made during the Mauna Loa Observatory Photochemistry Experiment 2, *J. Geophys. Res.*, 101, 14,729–14,739, 1996.

Stevens, B., G. Feingold, W. R. Cotton, and R. L. Walko, Elements of the microphysical structure of numerically simulated stratocumulus, *J. Atmos. Sci.*, 53, 980–1006, 1996.

Talbot, R. W., et al., Chemical characteristics of continental outflow from Asia to the troposphere over the western Pacific Ocean during September-October 1991: Results from PEM-West A, *J. Geophys. Res.*, 101, 1713–1725, 1996.

Tang, I. N., and J. H. Lee, Accomodation coefficients of ozone and SO_2: Implications on SO_2 oxidation in cloud water, in *The Chemistry of Acid Rain: Sources and Atmospheric Processes, Symp. Ser.,*vol. 349, edited by R. W. Johnson et al., pp. 109–117, Am. Chem. Soc., Washington, D. C., 1987.

Thomas, K., D. Kley, D. Mihelcic, and A. Volz-Thomas, Mass accomodation coefficient for NO_3 radicals on water: Implication for atmospheric

oxidation processes, paper presented at International Conference on the Generation of Oxidants on Regional and Global Scales, Univ. of East Anglia, Norwich, England, 3–7 July, 1989.

Thompson, A. M., and R. J. Cicerone, Possible perturbations to atmospheric CO, CH$_4$, and OH, *J. Geophys. Res.*, *91*, 10,853–10,864, 1986.

Thompson, A. M., et al., Ozone observation and a model of marine boundary photochemistry during SAGA 3, *J. Geophys. Res.*, *98*, 16,955–16,968, 1993.

Tremmel, H. G., W. Junkermann, F. Slemr, and U. Platt, On the distribution of hydrogen peroxide in the lower troposphere over the northern United States during late summer of 1988, *J. Geophys. Res.*, *98*, 1083–1099, 1993.

Walcek, C. J., H.-H. Yuan, and W. R Stockwell, The influence of aqueous-phase chemical reactions on ozone formation in polluted and nonpolluted clouds, *Atmos. Environ.*, *31*, 1221–1237, 1997.

Weeks, J. L., and J. Rabini, The pulse radiolysis of deaerated aqueous carbonate solutions, *J. Phys. Chem.*, *70*, 2100–2106, 1966.

Weinstein, J., and B. H. Bielski, Kinetics of the interaction of HO$_2$ and O$_2^-$ radicals with hydrogen peroxide: The Haber-Weiss reaction, *J. Am. Chem. Soc.*, *101*, 58–62, 1979.

Weinstein-Lloyd, J. B., J. H. Lee, P. H. Daum, L. I. Kleinman, L. J. Nunnermacker, S. R. Springton, and L. Newman, Measurements of peroxides and related species during the 1995 summer intensive of the Southern Oxidants Study in Nashville, Tennessee, *J. Geophys. Res.*, *103*, 22,361–22,373, 1998.

Zhang, Y., S. M. Kreidenweis, and G. Feingold, Stratocumulus processing of gases and cloud condensation nuclei, 2, Chemistry sensitivity analysis, *J. Geophys. Res.*, *104*, 16,061–16,080, 1999.

————————

G. Feingold, Environmental Technology Laboratory, NOAA, Boulder, CO 80305, USA.

G. J. Frost and M. K. Trainer, Aeronomy Laboratory, NOAA, Boulder, CO 80305, USA.

C.-H. Kim and S. M. Kreidenweis (corresponding author), Department of Atmospheric Science, Colorado State University, Fort Collins, CO 80523, USA. (soniak@aerosol.atmos.colostate.edu)